Supplemental Data 2 for "Problematic putative pachycephalosaurids: Synchrotron μCT imaging shines new light on the anatomy and taxonomic validity of *Gravitholus albertae* from the Belly River Group (Campanian) of Alberta, Canada"

Contents:

1. Corrected Measurements

Schott et al. (2011) reported a frontoparietal thickness of 49.6mm for CMN 1108(A) (a cast of the original), whereas Brown and Schlaikjer (1943) reported a frontoparietal thickness of 36 mm from the original specimen. Examination of its published photographs (Brown and Schlaikjer, 1943) suggests that 36 mm is the correct frontoparietal thickness. The frontoparietal thickness for CMN 1108A reported by Schott et al. (2011) is identical to its reported frontoparietal width. No other pachycephalosaurid frontoparietal in this dataset is as thick as it is tall, except the unnumbered UCMZ(VP) specimen. Otherwise frontoparietal thickness does not exceed 80% of frontoparietal width. For that reason, the unnumbered UCMZ(VP) specimen was not included in PCA analyses.

Preliminary morphometric results using the measurements provided by Schott and Evans (2017) scored CMN 8817 (holotype of "*Hanssuesia sternbergi*") dissimilar from other specimens of "*Hanssuesia sternbergi*" and *Stegoceras validum*. We investigated the variables influencing the placement of CMN 8817, and identified W:Po/stf/Sq and L:Po as strongly influencing the placement of CMN 8817. By re-examining CMN 8817, we concluded that the posterior landmark for the sutural surface for the postorbital was likely misidentified by Schott and Evans (2017). The posterior extent of the postorbital (a landmark for both of these measurements) appears to have been identified at a dorsoventrally directed ridge along a continuous sutural surface that extends to the broken surface of the posterior portion of the parietal (Fig. S9B). Similar ridges present along the sutural surface for the postorbital in other specimens of *Hanssuesia* sternbergi, such as TMP 2000.026.0001 (Fig. S1B) and TMP 2017.012.0019 (Fig. S2B). In these specimens, the sutural surface for the postorbital continues posteriorly from this ridge, until it reaches the margin of the supratemporal fenestra.

As a sutural surface continues posteriorly on CMN 8817 from the landmark identified by Schott and Evans (2017) the logical conclusion based on their interpretation would be that this posterior sutural surface is for the parietal contact with the squamosal, and that the supratemporal fenestrae of CMN 8817 are closed. Previous descriptions and assessments of the supratemporal fenestrae in CMN 8817 and *Hanssuesia sternbergi* at large vary. While the supratemporal fenestrae were not described by Brown and Schlaikjer (1943), they do describe a parietosquamosal shelf from CMN 192 and CMN 8817 (presumably considering the temporal region preserved). However, they reported a number of frontoparietal length measurements for specimens that do not preserve the median extension of the parietal (e.g., AMNH 5388, CMN 1108, and CMN 8818), as is the condition in CMN 192 and CMN 8817. Williamson and Carr (2002) assessed CMN 8817 with a caudal margin of the dome perpendicular to a parietosquamosal shelf (ch51[2]) as opposed to blending with the shelf, which contradicts the preserved depressed parietal region of the dome (Brown and Schlaikjer 1943; Sullivan 2003). Sullivan (2003) largely relied on his referral of UCMP 130051 to *Hanssuesia sternbergi* when describing the supratemporal fenestrae and sutural surface for the squamosal for this taxon. UCMP 130051 has since been referred to *Stegoceras* sp. (Schott and Evans 2012; see main text for discussion on the taxonomic identity of UCMP 130051). Maryańska et al. (2004) considered *Hanssuesia sternbergi* synonymous with *Stegoceras validum*, and assessed the latter as having closed supratemporal fenestrae (ch18[1]) in their phylogenetic analysis. Longrich et al. (2010) differentiated "*Texacephale langstoni*" from *Hanssuesia sternbergi* in that the former possessed open supratemporal fenestrae, and assessed the later as possessing closed supratemporal fenestrae (ch22[1]) in their phylogenetic analysis. Evans et al. (2013) assessed *Hanssuesia sternbergi* as possessing open supratemporal fenestrae (ch28[0]) in their phylogenetic analysis.

This assessment has been unaltered in subsequent studies (Schott and Evans 2017; Woodruff et al. 2021; Evans et al. 2021).

Unfortunately CMN 8817 is posteriorly damaged, missing the posterior extension of the parietal (Fig S9G). The dorsoventral thickness of the peripheral sutural surface along the parietal thins posteriorly (Figs. S9E-G), consistent with the posterior margin of the sutural surface for the postorbital immediately anterior to open supratemporal fenestrae. This also suggests that the posterior extent of the contact for the postorbital did not extend far beyond the preserved portion of the specimen, and that L:Po and W:Po/stf/Sq can be reasonably estimated. Therefore, we estimated W:Po/stf/Sq and L:Po. Morphometric analyses incorporating these corrected estimations score CMN 8817 like other *Hanssuesia sternbergi*.

The L:Po for ROM 58311 appeared as an outlier in preliminary initial RMA regressions. We re-examined the specimen and found that the posterior landmark for L:Po was likely misidentified, and is more posteriorly positioned than was measured by Schott et al. (2011). This measurement is preserved on the right side of the specimen, and was remeasured for this study.

CMN 515 appears to have a damaged endocranial roof along the frontoparietal suture, resulting in an apparent pinching in the endocranial roof along that contact (see photos in Jasinski and Sullivan, 2011). The W:endo has been re-estimated as 14.02 mm from Jasinski and Sullivan's (2011) photographs.

Schott and Evans (2017) reported frontal length and all peripheral frontoparietal heights for UALVP 8504 (identified as *Stegoceras validum*, though see Sullivan 2003 and Dyer et al. 2021 for referral to *Foraminacephale*). However, the specimen lacks the frontonasal boss, and

most of the supraorbital lobes (Dyer et al. 2021). Given these inconsistencies, all linear measurements were reassessed and re-measured for this study.

2. Reinterpretation of the Pachycephalosaurian Palpebral

After several interpretations of the number and names of the elements that make up the supraorbital region in pachycephalosaurians (see Sullivan, 2003 for historical interpretations), two supraorbital elements are currently recognised: the anterior supraorbital and posterior supraorbital. Maidment and Porro (2010) explored the homology of various ornithischian supraorbital to the plesiomorphic palpebral condition. They identified a similar topology between the pachycephalosaurian anterior supraorbital and the plesiomorphic ornithischian palpebral, where both contact the prefrontal anterolaterally (through posteriorly continuous in pachycephalosaurians), and the lacrimal anteroventrally, and speculated that the anterior supraorbital was a modified palpebral. However, Maidment and Porro (2010) stated the absence of basal pachycephalosaurians inhibited a test of primary homology (sensu de Pinna, 1991). Primary tests of homology (ie. Test of similarity sensu Patterson 1982) can be performed by comparing similarities in topology, development, and morphology between two taxa at any taxonomic level (de Pinna, 1991). We find no reason that a test of primary homology (similarity) between the plesiomorphic ornithischian palpebral and the pachycephalosaurid anterior supraorbital cannot be made, nor be followed by a test of congruence (secondary homology). The discovery of basal members can inspire further testing of the primary homology. Indeed, the recovery of heterodontosaurids, which retain palpebrals, as basal pachycephalosaurians (Dieudonné et al., 2020) meets this requirement.

Maidment and Porro (2010) perform the test of congruence by mapping the distribution of palpebrals and supraorbitals over phylogenetic trees of the major ornithischian clades, as a test primary homology. This did not test the primary homology assessments that a supraorbital element is homologous with the palpebral, but instead demonstrated the “homology” of

nomenclature. They identify character state changes of what is called the palpebral changing into what we call supraorbitals, despite previously demonstrating primary homology in several ornithischian groups. The correct test of congruence of the primary homology would be to assess taxa that possess supraorbitals that are similar (test of similarity) to the palpebral as palpebrals. Repeating the mapping exercise conducted by Maidment and Porro (2010), but treating the anterior supraorbital as a palpebral due to topological similarity, all ornithischians would possess palpebrals. What Maidment and Porro's (2010) test of congruence tested was the state that the palpebral covers the supraorbital region. In this case, they identify several convergences within Ornithischia of the palpebral incorporating with additional skull roof elements to dorsally close (ossify) the orbital margin. Pachycephalosaurians represent one of these independent convergent events, where the palpebral participates in closing the dorsal region of the orbit via a contact with the frontal and a de novo posterior supraorbital. Therefore, the pachycephalosaurian "anterior supraorbital" is referred to here as the palpebral.

3. Pathological Interpretations of CMN 9148

Peterson et al. (2013) were the first to perform a large survey of pachycephalosaurian cranial domes for osteopathologies, which they interpreted as consistent with posttraumatic infections resulting from intraspecific cranial combat. These pathological alterations wee described as pit-like depressions of various sizes, with smooth margins and irregular surface of the lesion floors. Multifocal specimens, with more than one lesion were, more common than single lesion specimens.

While CMN 9148 does not meet the diagnostic criteria provided by Peterson et al. (2013), the topography of the dorsal surface is unusual. The overall shape of the dome is asymmetrical, with the apex of the dome skewed to the left side (Figs. S10C, D). The dorsal surface is smoothed, but shallow depressions and grooves cover various regions, most notably the left supraorbital lobe (Fig. S10G). This resembles the floors of large, presumed multifocal lesions of other pathological frontoparietals (e.g., UALVP 8504; Dyer et al. 2021). The neurovascular foramina exiting the dorsal surface are enlarged relative to other specimens (e.g. TMP 2000.026.0001 Fig S1), and are more similar to other pathological specimens (e.g., TMP 1979.014.0853; Peterson et al. 2013). These abnormalities suggest advanced, extensive resorption to the dorsal surface. The absence of large lesions may be explained by continued growth after healing and recovering from the disease, or by complete fusion of multiple lesions covering the entire dorsal surface.

4. L:F and W:F/P Proportionate PCA of Belly River Group Pachycephalosaurians

PC loadings

Table S16 and S17 summarize the variable loading for the first four PC's of the L:F proportionate and W:F/P proportionate PCA respectively. PC 1 explained 61.9 % of the total variation in the L:F proportionate iteration, and 38.2% in the W:F/P proportionate matrix. All variables positively loaded on PC 1 of the L:F proportionate PCA. PC 1 of the L:F proportionate PCA was strongly loaded by W:F/P, W:Pso/Po. W:Po/stf/Sq, W:Pl/Pso, and T:F/P. PC 1 of the W:F/P proportionate PCA was strongly positively loaded by L:F, L:Po, and W:Prf/Pl,, and W:Po/stf/Sq was the variable that had the highest negative loading.

PC 2 explained 20.4% of the total variation in the L:F proportionate iteration. It was strongly positively loaded by H:N/N, T:F/P, and L:Po, and strongly negatively loaded by W:Po/stf/Sq. PC 2 explained 29.3% of the variance in the W:F/P proportionate iteration. It was strongly positively loaded by W:Po.stf.Sq, L:F, and W:Pl/Pso, and strongly negatively loaded by T:F/P.

PC 3 in the L:F proportionate iteration explained 5.1% of the total variance. It was strongly positively loaded by H:Pso/Po and W:Pso/Po, and strongly negatively loaded by T:F/P. PC 3 in the W:F/P proportionate iteration explained 10.7% of the total variance. It was strongly positively loaded by H:N/Prf, H:Pso/Po, H:N/N, and was strongly negatively loaded by L:F.

PC scorings

TMP 1972.027.0001 has the highest PC 1 and PC 2 scores amongst Belly River Group pachycephalosaurians in the L:F proportionate PCA (Fig. S4). All other pachycephalosaurian taxa overlap in PC 1, although there is little overlap between "*Hanssuesia sternbergi*" and

Stegoceras validum. *Foraminacephale brevis* is completely negatively separated from all other specimens in PC 2, whereas *Colepiocephale lambei*, "*Hanssuesia sternbergi*", and *Stegoceras validum* all extensively overlap with each other. TMP 1972.027.0001 scored within the range of "*Hanssuesia sternbergi*" and *Stegoceras validum* in PC 3. *Colepiocephale lambei* is completely negatively separated from other specimens in PC 3. *Foraminacephale brevis* mostly overlaps with "*Hanssuesia sternbergi*" and *Stegoceras validum* in PC 3. Pachycephalosaurian taxa all extensively overlapped in PC 4.

TMP 1972.027.0001 scored similar to *Colepiocephale lambei* and "*Hanssuesia sternbergi*" in PC 1 of the W:F/P proportionate PCA (Fig. S5). *Foraminacephale brevis* was negatively separated from "*Hanssuesia sternbergi*" and *Stegoceras validum*, but not entirely separated from *Colepiocephale lambei*. *Colepiocephale lambei* and "*Hanssuesia sternbergi*" slightly overlap with *Stegoceras validum*. TMP 1972.027.0001 scores similar to *Colepiocephale lambei* in PC 2. "*Hanssuesia sternbergi*" is negatively separated from *Foraminacephale brevis*. *Colepiocephale lambei* extensively overlaps with *Stegoceras validum*, but is almost negatively separated from *Foraminacephale brevis*. Pachycephalosaurian taxa all extensively overlap in PC 3. TMP 1972.027.0001 had the negative-most score in PC 4. *Colepiocephale lambei* is nearly positively separated from "*Hanssuesia sternbergi*", although both extensively overlap with *Foraminacephale brevis* and *Stegoceras validum*.

5. Influence of Transformation Methods on Frontoparietal Linear Measurement used in PCA

Previous PCAs of pachycephalosaurian linear frontoparietals measurements are typically performed on $\log_{10}$-transformed measurements (Evans et al. 2013; Williamson and Brusatte 2016; Schott and Evans 2017). Interestingly, the PCA performed in this study on non-transformed linear measurements were able to separate species better than in PCA based on $\log_{10}$-transformed measurements. This may be because $\log_{10}$-transformed the suite of frontoparietal measurements over emphasises variation in measurements that range below 10 mm (peripheral heights), whereas most other frontoparietal measurements range within a single order of magnitude (10-100 mm, except for three W:Pso/Po measurements) (Fig. S11). Furthermore, PC 1 was better explained by frontoparietal size in the non-transformed PCA than the $\log_{10}$-transformed PCA. Given that most measurements fall within a single order of magnitude, PCA based on non-transformed frontoparietal measurements may be more powerful than PCA based on $\log_{10}$-transformed measurements.

The PCA based on frontoparietal measurements proportioned to the length of the frontal resulted in the strongest taxonomic separation. Variable loadings were similar to the non-transformed PCA, but each subsequent axis after PC 1 explained more variation than in the non-transformed PCA. Conversely, the PCA based on frontoparietal measurements proportioned to the width of the frontoparietal contact resulted in poor taxonomic separation.

6. Supplementary Tables S6-24

Supplementary Tables S1-5 are provided in Supplementary Data File 1

Table S6. Bivariate analyses of endocranial size vs. frontoparietal size amongst Belly River Group pachycephalosaurians. Significant p values (< 0.05) are bolded.

	n	r^2	slope	ci	intercept	ci	p	allometry
W:F/P vs L:olf/soc	29	0.28	0.71	0.48 – 0.92	0.22	-0.16 – 0.65	**3.08 E-2**	-
L:F vs. L:olf/soc	26	0.45	0.99	0.64 – 1.24	-0.10	-0.51 – 0.50	**1.87 E-4**	ISO
W:F/P vs W:cer	41	0.18	0.38	0.26 – 0.50	0.61	0.41 – 0.84	**5.26 E-3**	-
L:F vs W:cer	36	0.05	0.62	0.31 – 0.89	0.29	-0.16 – 0.80	0.19	NA

Table S7. RMA regression results comparing frontoparietal widths to frontal length. Significant p values (< 0.05) are bolded.

	Taxon	n	r^2	slope	ci	intercept	ci	p
W:N/Prf	*Stegoceras validum*	34	0.42	1.57	1.14 – 1.90	-1.18	-1.73 – -0.49	**3.17 E-5**
	Hanssuesia sternbergi	6	0.18	2.88	-0.44 – 9.76	-3.42	-15.20 – 2.35	0.41
	S+H+G	41	0.57	1.71	1.39 – 2.01	-1.40	-1.89 – -0.87	**1.27 E-8**
	Colepiocephale lambei	13	0.55	1.13	0.30 – 1.47	-0.47	-1.03 – 0.94	**3.91 E-3**
	Foraminacephale brevis	16	0.64	1.67	0.80 – 2.13	-1.30	-1.99 – 0.03	**1.86 E-4**
	All	70	0.70	1.47	1.28 – 1.63	-1.00	-1.27 – -0.71	**2.31 E-19**
W:Pl/Pso	*Stegoceras validum*	35	0.50	1.13	0.85 – 1.36	-0.11	-0.47 – 0.36	**2.17 E-6**
	Hanssuesia sternbergi	6	0.50	1.22	0.10 – 2.01	-0.18	-1.55 – 1.76	0.11
	S+H+G	42	0.62	1.37	1.10 – 1.60	-0.49	-0.87 – -0.03	**6.13 E-10**
	Colepiocephale lambei	15	0.25	1.08	0.19 – 1.51	0.02	-0.70 – 1.52	0.06
	Foraminacephale brevis	15	0.67	1.15	0.64 – 1.50	-0.04	-0.58 – 0.74	**1.83 E-4**
	All	72	0.61	1.10	0.94 – 1.26	-0.03	-0.28 – 0.26	**4.52 E-16**
W:Po/stf/Sq	*Stegoceras validum*	20	0.69	1.39	1.00 – 1.66	-0.66	-1.12 – 0.01	**6.03 E-6**
	Hanssuesia sternbergi	5	0.60	2.17	0.54 – 6.27	-1.92	-9.00 – 0.94	0.12
	S+H+G	26	0.74	1.80	1.32 – 2.19	-1.32	-1.97 – -0.51	**1.82 E-8**
	Colepiocephale lambei	14	0.34	1.31	0.74 – 4.12	-0.47	-5.20 – 0.51	**0.03**
	Foraminacephale brevis	13	0.74	1.44	0.99 – 1.76	-0.47	-0.96 – 0.12	**1.68 E-4**
	All	53	0.26	1.09	0.78 – 1.31	-0.08	-0.45 – 0.44	**1.08 E-4**

Table S8. Tukey's Pairwise results comparing the average of W:Pl/Pso residuals between Belly River Group pachycephalosaurian taxa (excluding TMP 1972.027.0001). Significant p values (< 0.05) are bolded. Tukey's Q values are reported below the "x".

	Stegoceras validum	*Hanssuesia sternbergi*	*Foraminacephale brevis*	*Colepiocephale lambei*
Stegoceras validum	x	**5.58 E-3**	**1.28 E-5**	0.15
Hanssuesia sternbergi	4.85	x	1.00	0.30
Foraminacephale brevis	7.33	0.24	x	0.06
Colepiocephale lambei	3.02	2.51	3.64	x

Table S9. Tukey's Pairwise results comparing the average of W:Po/stf/Sq residuals between Belly River Group pachycephalosaurian taxa (excluding TMP 1972.027.0001). Significant p values (< 0.05) are bolded. Tukey's Q values are reported below the "x".

	Stegoceras validum	*Hanssuesia sternbergi*	*Foraminacephale brevis*	*Colepiocephale lambei*
Stegoceras validum	x	**3.56 E-4**	**0**	**4.77 E-3**
Hanssuesia sternbergi	6.20	x	**1.18 E-3**	0.27
Foraminacephale brevis	17.08	5.67	x	**1.48 E-09**
Colepiocephale lambei	5.01	2.60	11.26	x

Table S10. RMA regression results comparing supraorbital heights to frontoparietal thickness. Significant p values (< 0.05) are bolded.

	Taxon	n	r^2	slope	ci	intercept	ci	p
H:Prf/Pl	*Stegoceras validum*	42	0.84	0.94	0.82 – 1.05	-0.32	-0.49 – -0.14	**9.43 E-18**
	Hanssuesia sternbergi	8	0.23	2.81	0.15 – 7.77	-3.67	-12.72 – 1.08	0.23
	S+H+G	51	0.87	0.95	0.85 – 1.04	-0.34	-0.49 – -0.17	**2.92 E-23**
	Colepiocephale lambei	15	0.26	1.35	0.49 – 1.93	-1.16	-2.21 – 0.41	**0.05**
	Foraminacephale brevis	23	0.73	1.27	0.34 – 1.53	-0.93	-1.31 – 0.45	**1.75 E-7**
	All	89	0.79	0.98	0.86 – 1.07	-0.44	-0.58 - -0.24	**2.08 E-31**
H:Pl/Pso	*Stegoceras validum*	42	0.71	0.91	0.73 – 1.05	-0.39	-0.59 – -0.11	**3.08 E-12**
	Hanssuesia sternbergi	9	0.11	2.09	0.15 – 6.58	-2.43	-10.56 – 0.96	0.39
	S+H+G	52	0.78	0.97	0.81 – 1.09	-0.46	-0.66 – -0.20	**5.89 E-18**
	Colepiocephale lambei	14	0.24	1.11	0.57 – 1.60	-0.84	-1.70 – 0.17	0.07
	Foraminacephale brevis	25	0.74	1.62	1.08 – 2.24	-1.55	-2.45 – -0.79	**3.00 E-8**
	All	91	0.72	1.04	0.85 – 1.19	-0.62	-0.87 – -0.31	**3.41 E-26**
H:Pso/Po	*Stegoceras validum*	43	0.80	0.66	0.56 – 0.74	0.16	0.05 – 0.32	**6.06 E-16**
	Hanssuesia sternbergi	9	0.35	3.11	-0.03 – 5.03	-4.14	-7.63 – 1.41	0.09
	S+H+G	53	0.82	0.75	0.64 – 0.82	0.06	-0.06 – 0.22	**1.21 E-20**
	Colepiocephale lambei	13	0.53	1.63	0.86 – 2.24	-1.71	-2.75 – -0.35	**4.62 E-3**
	Foraminacephale brevis	31	0.44	1.15	0.68 – 1.37	-0.56	-0.87 – 0.12	**5.43 E-5**
	All	97	0.63	0.76	0.64 – 0.84	0.01	-0.12 – 0.18	**1.90 E-22**

Table S11. Tukey's Pairwise results comparing the average of H:Prf/Pl residuals between Belly River Group pachycephalosaurian taxa (excluding TMP 1972.027.0001). Significant p values (< 0.05) are bolded. Tukey's Q values are reported below the "x".

	Stegoceras validum	*Hanssuesia sternbergi*	*Foraminacephale brevis*	*Colepiocephale lambei*
Stegoceras validum	x	1	**2.77 E-05**	**4.80 E-4**
Hanssuesia sternbergi	0.24	x	**0.02**	**0.04**
Foraminacephale brevis	6.92	4.15	x	1
Colepiocephale lambei	5.85	3.80	0.11	x

Table S12. Tukey's Pairwise results comparing the average of H:Pl/Pso residuals Between Belly River Group pachycephalosaurian taxa (excluding TMP 1972.027.0001). Significant p values (< 0.05) are bolded. Tukey's Q values are reported below the "x".

	Stegoceras validum	*Hanssuesia sternbergi*	*Foraminacephale brevis*	*Colepiocephale lambei*
Stegoceras validum	x	0.96	**2.32 E-3**	**0.01**
Hanssuesia sternbergi	0.67	x	**0.03**	**0.04**
Foraminacephale brevis	5.19	4.01	x	1
Colepiocephale lambei	4.51	3.83	0.23	x

Table S13. Tukey's Pairwise results comparing the average of H:Pso/Po residuals between Belly River Group pachycephalosaurian taxa (excluding TMP 1972.027.0001). Significant p values (< 0.05) are bolded. Tukey's Q values are reported below the "x".

	Stegoceras validum	*Hanssuesia sternbergi*	*Foraminacephale brevis*	*Colepiocephale lambei*
Stegoceras validum	x	0.70	0.98	**9.99 E-07**
Hanssuesia sternbergi	1.54	x	0.56	**1.29 E-05**
Foraminacephale brevis	0.56	1.84	x	**9.05 E-06**
Colepiocephale lambei	8.01	7.15	7.27	x

Table S14. PC loadings of the PCA based on log_{10}-transformed linear measurements of Belly River Group frontoparietals. Variables that load > |0.3| are bolded.

	PC 1 (72.6%)	PC 2 (6.5%)	PC 3 (5.0%)	PC 4 (2.6%)
H:N/N	**0.45324**	**-0.37633**	0.020288	0.18046
H:N/Prf	**0.37201**	-0.25369	**-0.6657**	0.28705
H:Prf/Pl	**0.33117**	-1.94E-05	-0.0323	-0.21382
H:Pl/Pso	**0.31655**	0.073464	0.036335	**-0.78128**
H:Pso/Po	0.17453	**0.30421**	**-0.38173**	-0.23104
W:N/Prf	0.25433	-0.09268	0.14912	0.000951
W:Prf/Pl	0.19687	-0.048	0.29991	0.076019
W:Pl/Pso	0.18532	0.16356	0.14054	0.046624
W:Pso/Po	0.19488	0.13263	0.11113	0.038641
W:Po/stf/Sq	0.13439	**0.41509**	0.088056	0.13229
L:Pl	0.20462	**0.48201**	-0.21564	0.12722
L:Pso	0.11794	**0.41133**	0.11173	0.2771
L:Po	0.25291	-0.19465	0.22388	-0.02142
L:F	0.15234	-0.12902	0.21533	0.009414
T:F/P	0.28118	0.11175	**0.31755**	0.23468

Table S15. PC loadings of the PCA based on non-transformed linear measurements of Belly River Group frontoparietals. Variables that load > |0.3| are bolded.

	PC 1(84.2%)	PC 2 (5.6%)	PC 3 (2.9%)	PC 4 (2.4%)
H:N/N	0.22998	-0.19213	0.18321	**0.38304**
H:N/Prf	0.15059	-0.09292	**0.3544**	**0.44305**
H:Prf/Pl	0.15512	-0.02548	0.16602	0.18541
H:Pl/Pso	0.12537	-0.01295	0.16683	0.032502
H:Pso/Po	0.10858	0.20049	**0.36964**	0.070298
W:N/Prf	0.20192	-0.12367	0.20253	-0.02746
W:Prf/Pl	0.28227	-0.20981	-0.15465	**-0.42227**
W:Pl/Pso	**0.39131**	0.067955	-0.05775	-0.05541
W:Pso/Po	**0.46062**	0.1439	0.26892	-0.21967
W:Po/stf/Sq	0.2614	**0.74748**	-0.07459	-0.16821
L:Pl	0.10022	0.094748	0.1006	0.18633
L:Pso	0.10351	0.23348	-0.21607	0.2354
L:Po	0.28731	**-0.33579**	0.16102	-0.29371
L:F	0.20836	-0.29197	-0.17524	-0.14033
T:F/P	**0.41482**	-0.09267	**-0.62387**	**0.40229**

Table S16. PC loadings of the PCA based on L:F proportionate measurements of Belly River Group frontoparietals. Variables that load > |0.3| are bolded.

	PC 1 (61.9%)	PC 2 (20.6%)	PC 3 (5.1%)	PC 4 (3.9%)
H:N/N	0.12823	**0.41069**	0.12785	**0.32493**
H:N/Prf	0.10496	0.23994	0.24382	**0.36669**
H:Prf/Pl	0.10215	0.17178	0.16982	0.27083
H:Pl/Pso	0.092026	0.1333	0.17864	0.0709
H:Pso/Po	0.1487	-0.09922	**0.36547**	0.17337
W:N/Prf	0.099473	0.18644	0.23678	0.099748
W:Prf/Pl	0.14406	0.12388	-0.00152	**-0.448**
W:Pl/Pso	**0.34851**	-0.05326	0.086813	-0.11466
W:Pso/Po	**0.42135**	-0.00487	**0.34176**	-0.215
W:F/P	**0.51171**	0.046032	-0.29953	-0.09973
W:Po/stf/Sq	**0.41969**	**-0.59187**	0.035495	0.13675
L:Pl	0.12199	-0.03968	0.09804	0.15627
L:Pso	0.16944	-0.25406	-0.17874	0.17682
L:Po	0.14914	**0.33556**	0.16448	**-0.50425**
T:F/P	**0.31315**	**0.36405**	**-0.62441**	0.20713

Table S17. PC loadings of the PCA based on W:F/P proportionate measurements of Belly River Group frontoparietals. Variables that load > |0.3| are bolded.

	PC 1 (38.2%)	PC 2 (29.3%)	PC 3 (10.7%)	PC 4 (5.2%)
H:N/N	0.27025	-0.28809	**0.34413**	0.076915
H:N/Prf	0.19159	-0.11971	**0.36552**	0.006626
H:Prf/Pl	0.18004	-0.05214	0.29917	0.12218
H:Pl/Pso	0.1412	-0.02738	0.25203	-0.00313
H:Pso/Po	0.040135	0.20064	**0.36156**	-0.06317
W:N/Prf	0.27341	0.014153	0.14651	0.032439
W:Prf/Pl	**0.35738**	0.13456	-0.29504	0.006695
W:Pl/Pso	0.22613	**0.30581**	0.12365	0.0253
W:Pso/Po	0.26545	0.27958	0.24712	-0.18961
W:Po/stf/Sq	-0.27478	**0.57352**	0.24939	0.18076
L:Pl	-0.00275	0.093287	0.24465	-0.00271
L:Pso	-0.12289	0.23227	0.013596	**0.34984**
L:Po	**0.3979**	-0.09437	-0.10314	**-0.42276**
L:F	**0.49225**	**0.37777**	**-0.38145**	**0.30395**
T:F/P	0.14479	**-0.35464**	0.031194	**0.71501**

Table S18. RMA regressions of PC scores from the log_{10}-transformed PCA vs W:F/P.

Significant p values (< 0.05) are bolded.

	Taxon	n	r^2	slope	ci	intercept	ci	p
PC 1	*Stegoceras validum*	19	0.85	3.63	2.99 – 4.37	-6.40	-7.66 – -5.25	**1.58 E-8**
	Hanssuesia sternbergi	5	0.63	6.17	-3.55 – 12.19	-11.54	-23.56 – 7.46	0.11
	S+H+G	25	0.90	3.55	3.12 – 3.94	-6.28	-6.99 – -5.50	**6.39 E-13**
	Colepiocephale lambei	7	0.86	5.54	0.94 – 6.92	-10.33	-12.89 – -1.24	**2.76 E-3**
	Foraminacephale brevis	11	0.91	4.95	3.76 – 6.00	-9.11	-10.88 – -7.06	**5.74 E-6**
	All	43	0.82	4.25	3.72 – 4.76	-7.69	-8.65 – -6.72	**9.56 E-17**
PC 2	*Stegoceras validum*	19	0.43	1.10	0.53 – 1.60	-2.06	-2.93 – -1.03	**2.45 E-3**
	Hanssuesia sternbergi	5	0.39	2.54	0.51 – 9.65	-4.94	-18.85 – -0.85	0.26
	S+H+G	25	0.62	1.00	0.68 – 1.31	-1.89	-2.46 – -1.31	**3.39 E-6**
	Colepiocephale lambei	7	0.02	0.81	-4.74 – 1.60	-1.58	-3.08 – 9.19	0.77
	Foraminacephale brevis	11	0.20	0.90	-0.51 – 1.38	-1.38	-2.21 – 1.00	0.16
	All	43	0.07	1.22	0.86 – 3.46	-2.20	-6.32 – -1.59	0.09
PC 3	*Stegoceras validum*	19	0.03	0.58	0.24 – 1.85	-1.06	-3.30 – -0.49	0.45
	Hanssuesia sternbergi	5	0.07	-4.92	-16.12 – 5.32	9.78	-10.18 – 31.9	0.67
	S+H+G	25	0.10	0.65	0.44 – 1.87	-1.21	-3.40 – -0.85	0.13
	Colepiocephale lambei	7	0.67	-3.42	-4.68 – 2.06	6.73	-3.88 – 9.08	**0.02**
	Foraminacephale brevis	11	0.20	-0.83	-2.49 – 0.19	1.39	-0.36 – 4.28	0.17
	All	43	0.05	1.06	0.63 – 3.18	-1.93	-5.76 – -1.17	0.15
PC 4	*Stegoceras validum*	19	0.14	1.09	0.44 – 2.79	-1.92	-4.90 – -0.80	0.11
	Hanssuesia sternbergi	5	0.15	-3.04	-9.26 – 0.11	5.95	-0.38 – 18.19	0.52
	S+H+G	25	0.01	0.78	0.44 – 2.49	-1.42	-4.55 – -0.84	0.59
	Colepiocephale lambei	7	0.63	1.65	-0.51 – 6.56	-3.13	-12.67 – 0.98	**0.03**
	Foraminacephale brevis	11	0.01	1.10	0.16 – 3.82	-1.88	-6.53 – -0.25	0.74
	All	43	0.02	0.77	0.55 – 2.39	-1.40	-4.34 – -1.01	0.35

Table S19. RMA regressions of PC scores from the non-transformed PCA vs W:F/P.

Significant p values (< 0.05) are bolded.

	Taxon	n	r^2	slope	ci	intercept	ci	p
PC 1	*Stegoceras validum*	19	0.96	1.9	1.69 – 2.14	-124.95	-135.50 – -109.73	**4.41 E-13**
	Hanssuesia sternbergi	5	0.90	2.42	1.46 – 3.95	-173.20	-290.86 – -83.38	**0.01**
	S+H+G	25	0.97	1.83	1.69 – 1.95	-117.79	-125.81 – -109.23	**1.29 E-19**
	Colepiocephale lambei	7	0.85	1.62	1.22 – 4.68	-111.23	-377.81 – -8087	**3.17 E-3**
	Foraminacephale brevis	11	0.98	1.95	1.72 – 2.17	-137.85	-149.63 – -125.53	**9.20 E-9**
	All	43	0.95	1.89	1.75 – 2.03	-127.11	-136.19 – -118.17	**1.21 E-27**
PC 2	*Stegoceras validum*	19	0.28	0.21	0.02 – 0.31	-19.27	-25.86 – -9.34	**0.02**
	Hanssuesia sternbergi	5	0.34	0.81	0.16 –2.99	-82.75	-270.15 – -6.74	0.30
	S+H+G	25	0.56	0.26	0.17 – 0.35	-22.24	-28.18 – -16.57	**1.62 E-5**
	Colepiocephale lambei	7	0.05	0.61	-0.57 – 3.51	-54.42	-304.62 – 63.24	0.62
	Foraminacephale brevis	11	0.87	0.64	0.21 – 0.73	-22.49	-28.13 – -1.42	**2.87 E-5**
	All	43	0.01	0.49	0.33 – 1.53	-32.85	-103.90 – -23.85	0.52
PC 3	*Stegoceras validum*	19	0.05	-0.20	-0.68 – -0.07	14.74	7.74 – 42.26	0.35
	Hanssuesia sternbergi	5	0.26	1.15	-1.94 – 3.28	-104.21	-311.97 – 170.16	0.38
	S+H+G	25	0.05	0.21	0.16 – 0.67	-11.04	-41.10 – -6.57	0.27
	Colepiocephale lambei	7	0.05	0.59	-0.52 – 2.54	-60.85	-224.92 – 38.94	0.64
	Foraminacephale brevis	11	0.01	0.17	-0.09 – 0.72	-10.16	-39.33 – 2.36	0.78
	All	43	0.01	-0.35	-1.09 – -0.25	23.62	17.05 – 74.23	0.53
PC 4	*Stegoceras validum*	19	0.07	0.27	0.16 – 0.97	-16.00	-54.93– -9.17	0.26
	Hanssuesia sternbergi	5	0.02	1.66	0.23 – 5.81	-163.79	-567.14 – -39.90	0.83
	S+H+G	25	0.06	-0.29	-0.89 – -0.20	18.51	11.47 – 58.21	0.26
	Colepiocephale lambei	7	0.63	0.83	-0.27 – 1.27	-66.51	-100.35 – 34.77	**0.03**
	Foraminacephale brevis	11	0.16	0.21	0.00 – 0.94	-10.18	-47.79 – -1.57	0.22
	All	43	0.00	0.32	0.23– -1.02	-21.45	-69.05 – -15.08	0.89

Table S20. PC loadings of log_{10}-transformed measurements excluding *Colepiocephale lambei* and *Foraminacephale brevis*.

	PC 1 (81.2%)	PC 2 (4.2%)	PC 3 (4.2%)
H:N/N	**0.35082**	**0.34299**	0.002972
H:N/Prf	0.29778	**0.53724**	-0.26806
H:Prf/Pl	**0.30064**	-0.07149	-0.24802
H:Pl/Pso	**0.32882**	**-0.40093**	**-0.65105**
H:Pso/Po	0.23615	-0.03493	-0.23527
W:N/Prf	0.24415	0.056029	0.1188
W:Prf/Pl	0.19501	0.034558	0.28647
W:Pl/Pso	0.22065	-0.1455	0.19323
W:Pso/Po	0.23364	-0.02223	0.16637
W:Po/stf/Sq	0.22343	-0.11313	0.29632
L:Pl	**0.30114**	**-0.57727**	0.26148
L:Pso	0.20507	0.10737	0.10108
L:Po	0.2307	0.063249	0.11884
L:F	0.10877	0.035143	0.1317
T:F/P	0.29214	0.19454	0.16836

Table S21. PC loadings of non-transformed measurements excluding *Colepiocephale lambei* and *Foraminacephale brevis*.

	PC 1 (89.9%)	PC 2 (2.9%)	PC 3 (1.8%)
H:N/N	0.19563	**0.42303**	0.062779
H:N/Prf	0.13561	**0.51284**	0.1214
H:Prf/Pl	0.14259	0.21266	0.05912
H:Pl/Pso	0.12601	0.12076	-0.13925
H:Pso/Po	0.13043	0.19501	-0.20005
W:N/Prf	0.18926	0.093201	-0.19087
W:Prf/Pl	0.26671	-0.25441	**0.36235**
W:Pl/Pso	**0.40635**	-0.23201	**0.33044**
W:Pso/Po	**0.49371**	-0.04341	**-0.41594**
W:Po/stf/Sq	**0.32876**	**-0.47314**	-0.1107
L:Pl	0.11773	0.029704	**0.30066**
L:Pso	0.12724	0.13491	**0.40875**
L:Po	0.27335	-0.04953	**-0.34454**
L:F	0.14929	-0.08774	0.27849
T:F/P	**0.37302**	0.27924	0.049912

Table S22. PC loadings of L:F proportionate measurements excluding *Colepiocephale lambei* and *Foraminacephale brevis*.

	PC 1 (82.0%)	PC 2 (4.7%)	PC 3 (3.4%)
H:N/N	0.19669	**0.45149**	-0.00411
H:N/Prf	0.13123	**0.50643**	-0.14605
H:Prf/Pl	0.12542	0.2797	**0.30427**
H:Pl/Pso	0.12819	0.1513	**0.30796**
H:Pso/Po	0.11772	0.20797	0.16257
W:N/Prf	0.16896	0.1199	0.18538
W:Prf/Pl	0.19956	-0.22738	-0.10025
W:Pl/Pso	**0.3304**	-0.18011	**0.47578**
W:Pso/Po	**0.44025**	-0.08362	0.027521
W:F/P	**0.50047**	-0.18351	**-0.34958**
W:Po/stf/Sq	0.26057	**-0.39534**	0.23474
L:Pl	0.10323	0.055941	**0.36684**
L:Pso	0.08667	0.15685	-0.01971
L:Po	0.2428	-0.10831	**-0.3167**
T:F/P	**0.36226**	0.2457	-0.28407

Table S23. PC loadings of W:F/P proportionate measurements excluding *Colepiocephale lambei* and *Foraminacephale brevis*.

	PC 1 (45.5%)	PC 2 (16.0%)	PC 3 (10.8%)
H:N/N	-0.05933	**0.42881**	0.15654
H:N/Prf	0.005378	**0.31262**	**0.35482**
H:Prf/Pl	0.078555	**0.35466**	-0.04232
H:Pl/Pso	0.049526	**0.33078**	-0.15033
H:Pso/Po	0.13042	0.20352	-0.00514
W:N/Prf	0.12846	0.22615	-0.13186
W:Prf/Pl	0.29634	-0.13325	0.10097
W:Pl/Pso	**0.38206**	0.19688	**-0.38122**
W:Pso/Po	0.25828	0.22842	-0.09218
W:Po/stf/Sq	0.28153	-0.00479	**-0.40069**
L:Pl	0.061011	0.19433	**-0.31772**
L:Pso	0.15702	0.081999	0.20788
L:Po	0.10958	-0.03401	0.24214
L:F	**0.72637**	-0.21351	**0.38268**
T:F/P	-0.08102	**0.43667**	**0.36604**

Table S24. Length of the frontal-palpebral contact in select pachycephalosaurian specimens. Brackets following L:Pl measurements indicate the character state assessment of character 31.

Specimen	Taxon	W:F/P (mm)	L:Pl (mm)	Reference
CMN 8830	*Sphaerotholus edmontonensis*	66.00	11.6 (31[2])	Woodruff et al. (2021)
UWBM 89701	*Sphaerotholus buchholtzae*	66.60	5.5 (31[1]))	Woodruff et al. (2021)
TMP 1983.067.0001	*Stegoceras validum*	66.80	12.5 (31[2])	Schott and Evans (2017)
UALVP 31471	*Colepiocephale lambei*	68.65	14.87 (31[2])	This Study
TMP 2008.045.0001	*Acrotholus audeti*	70.10	8.6 (31[1])	Evans et al. (2013)
ROM 2964	*Acrotholus audeti*	85.52	16.06 (31[2])	This Study
NMMNH P-27403	*Sphaerotholus goodwini*	101.00	17.9 (31[2])	Evans et al. (2013)
CMN 8817	*Stegoceras validum*	102.50	20.3 (31[2])	Schott and Evans (2017)
Z. Pal. MgD-1/104	*Prenocephale prenes*	108.00	5 (31[1])	Evans et al. (2018)

7. Supplementary Figures

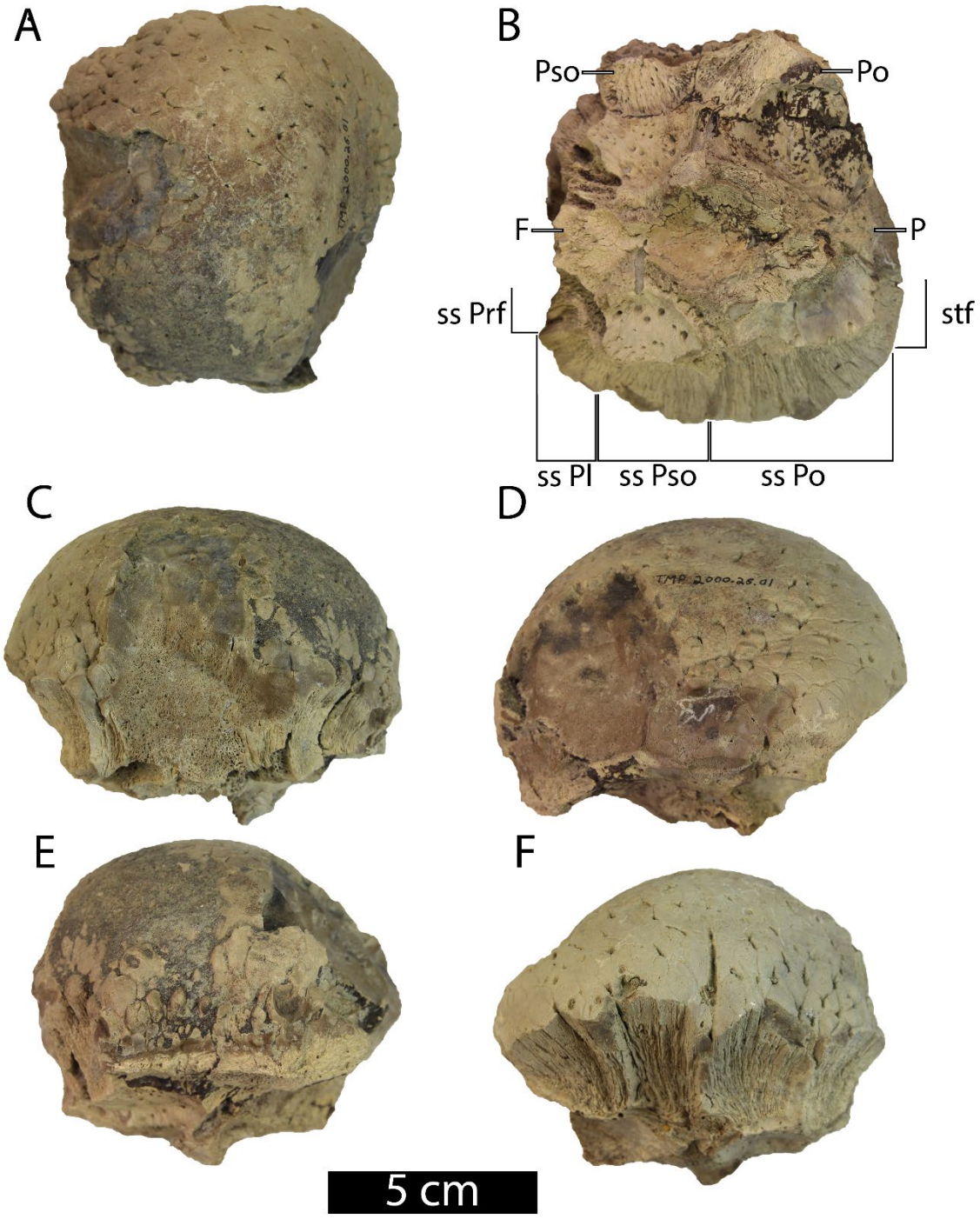

Figure S1. TMP 2000.026.0001 - incomplete skull roof of "*Hanssuesia sternbergi*" (= *Stegoceras validum*). The specimen contains a partial frontoparietal, left posterior supraorbital

and postorbital, and neurocranial elements A) Dorsal view. B) Ventral view. C) Anterior view. D) Posterior view. E) Left lateral view. F) Right lateral view. Abbreviations: F, frontals; P, parietal; Po, postorbital; Pso; posterior supraorbital; ss Pl, sutural surface for the palpebral; ss Po, sutural surface for the postorbital; ss Prf, sutural surface for the prefrontal; ss Pso, sutural surface for the posterior supraorbital; stf, supratemporal fenestra.

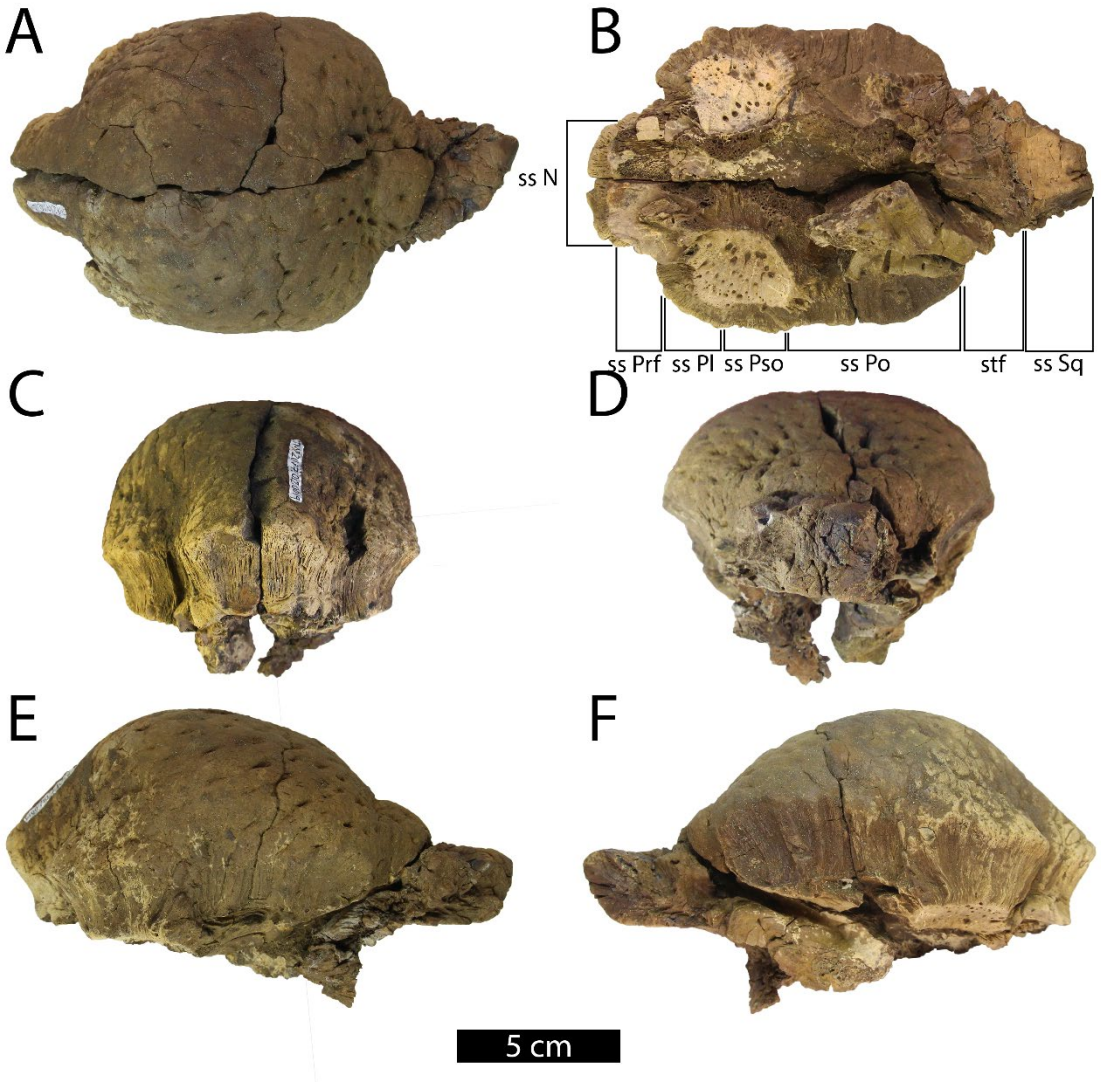

Figure S2. TMP 2017.012.0019 - complete frontoparietal dome of "*Hanssuesia sternbergi*" (= *Stegoceras validum*). A) Dorsal view. B) Ventral view. C) Anterior view. D) Posterior view. E) Left lateral view. F) Right lateral view. Abbreviations: ss N, sutural surface for the nasals; ss Pl, sutural surface for the palpebral; ss Po, sutural surface for the postorbital; ss Prf, sutural surface for the prefrontal; ss Pso, sutural surface for the posterior supraorbital; ss Sq, sutural surface for the squamosal; stf, supratemporal fenestra.

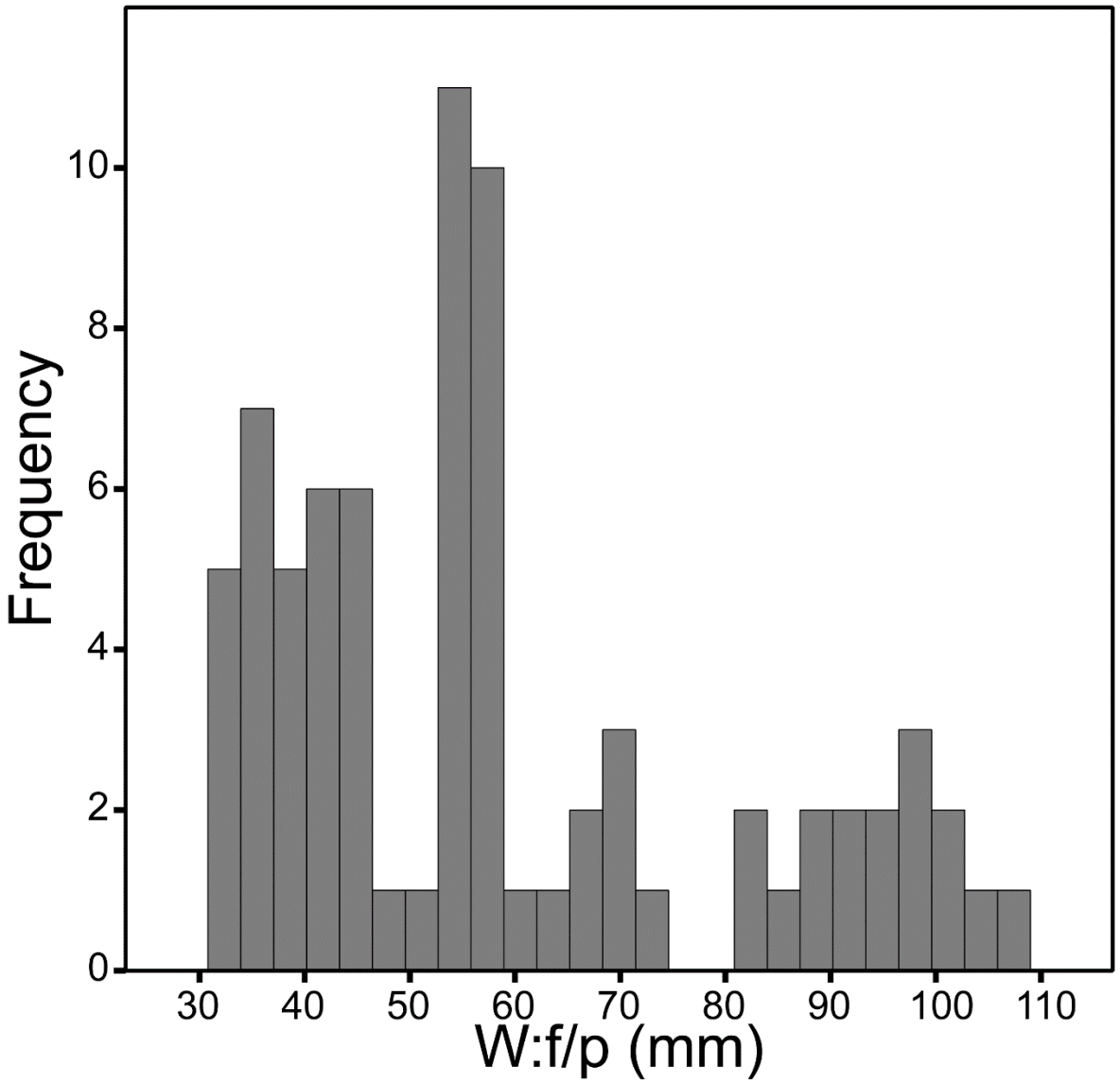

Figure S3. Size distribution of *Stegoceras validum* frontoparietals from the Belly River Group. Note the gap in the distribution around 80 mm.

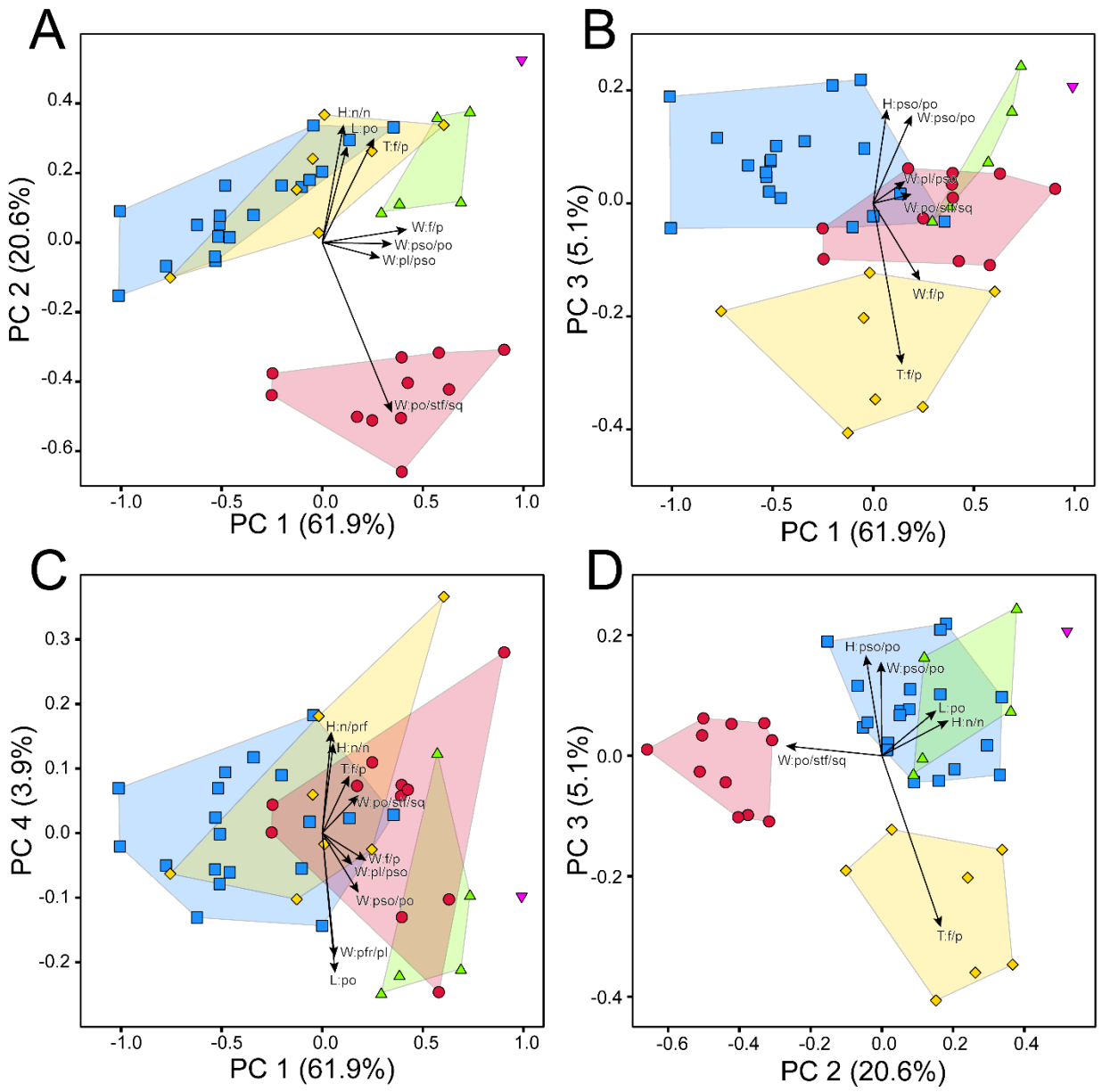

Figure S4. PCA of linear measurements proportionate to the length of the frontal. Purple inverted triangle – TMP 1972.027.0001; blue squares – *Stegoceras validum*; green triangles – *Hanssuesia sternbergi*; yellow diamonds – *Colepiocephale lambei*; red circles – *Foraminacephale brevis*. Arrows indicate eigenvectors of variables; only variables that loaded at least |0.3| in either axis are displayed.

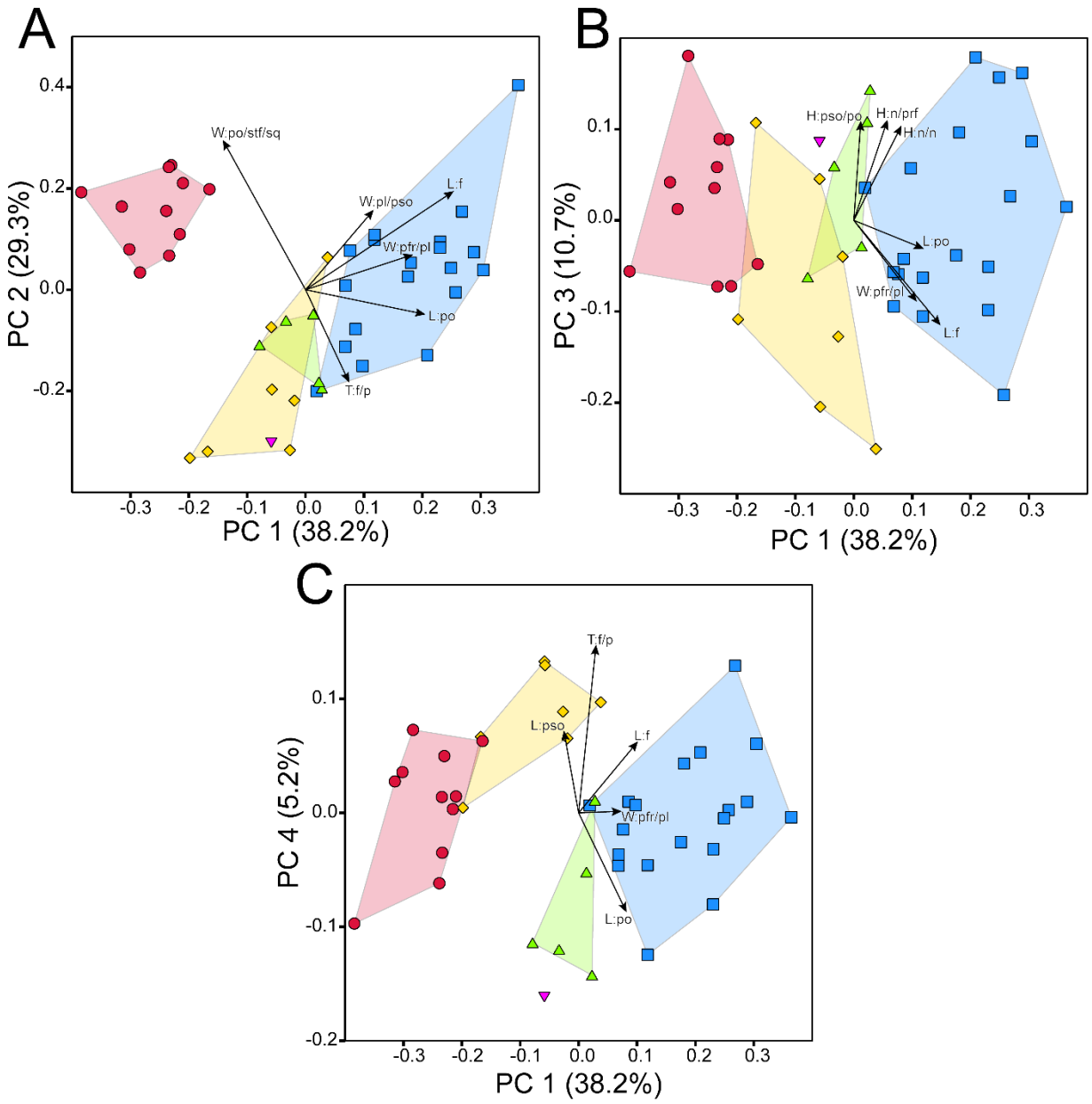

Figure S5. PCA of linear measurements proportionate to the width across the frontoparietal contact. Purple inverted triangle – TMP 1972.027.0001; blue squares – *Stegoceras validum*; green triangles – *Hanssuesia sternbergi*; yellow diamonds – *Colepiocephale lambei*; red circles – *Foraminacephale brevis*.

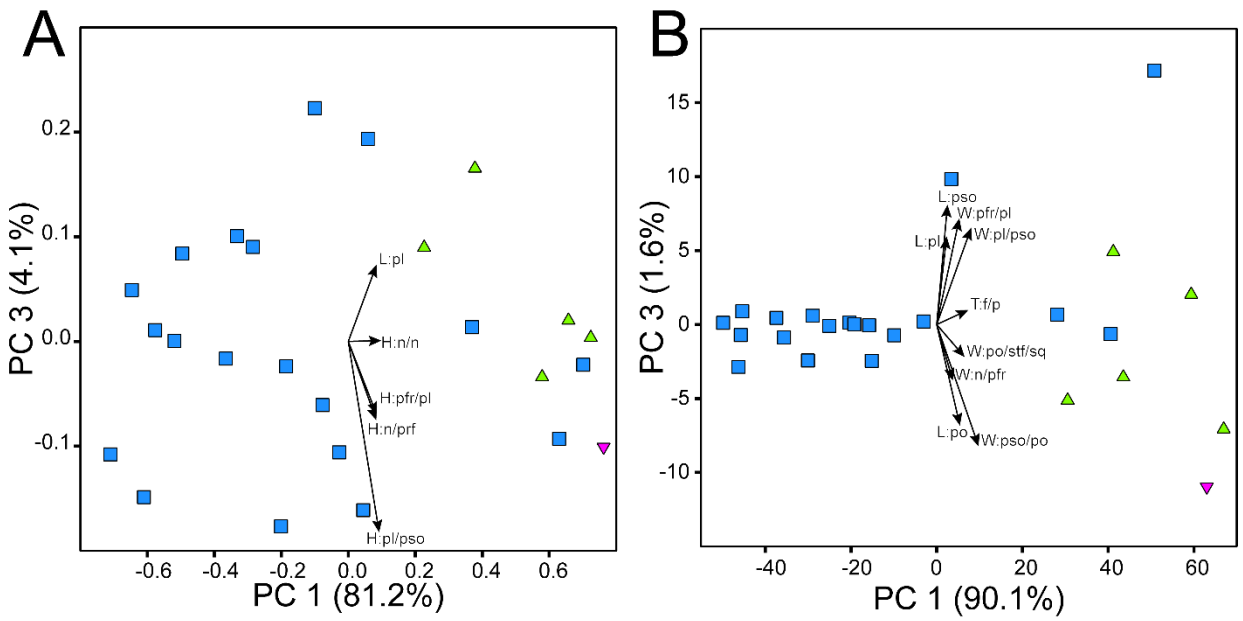

Figure S6. Additional PCA results from the non-transformed and $\log_{10}$-transformed iterations of TMP 1972.027.0001, "*Hanssuesia sternbergi"*, and *Stegoceras validum*. A) PC 1 vs. PC 3 of the log10-transformed iteration. B) PC 1 vs. PC 3 of the non-transformed iteration. Purple inverted triangle – TMP 1972.027.0001; blue squares – *Stegoceras validum*; green triangles – "*Hanssuesia sternbergi"*.

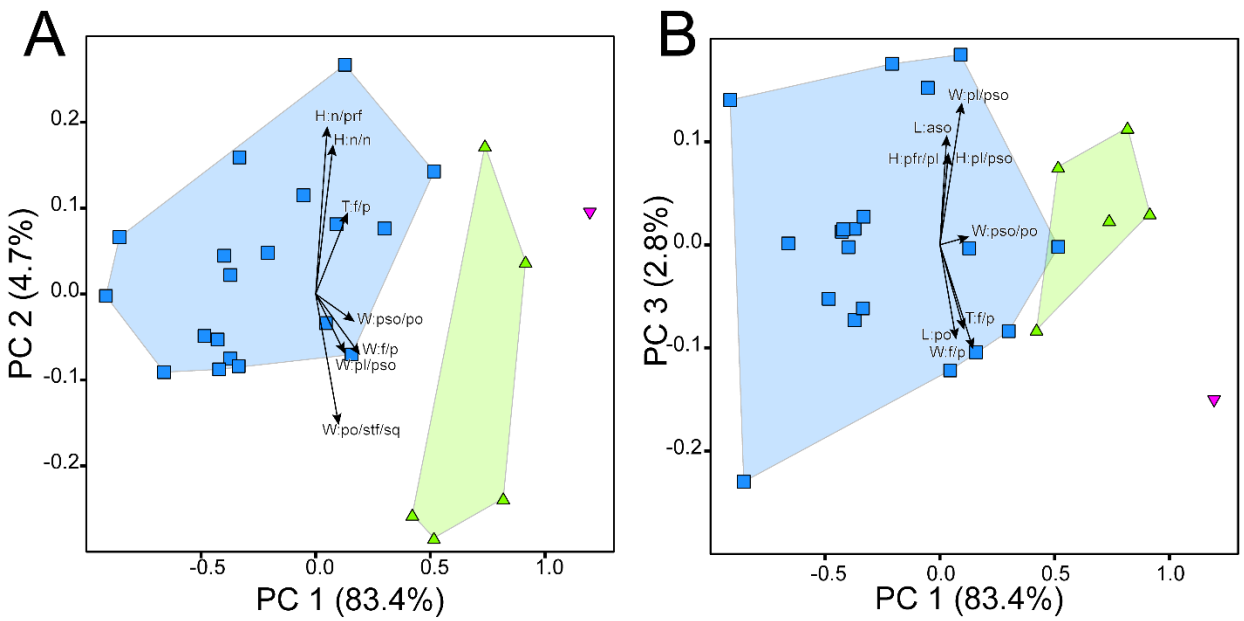

Figure S7. PCA of linear frontoparietal measurements proportionate to the length of the frontal. TMP 1972.027.0001, *"Hanssuesia sternbergi"*, and *Stegoceras validum*. Purple inverted triangle – TMP 1972.027.0001; blue squares – *Stegoceras validum*; green triangles – "*Hanssuesia sternbergi"*.

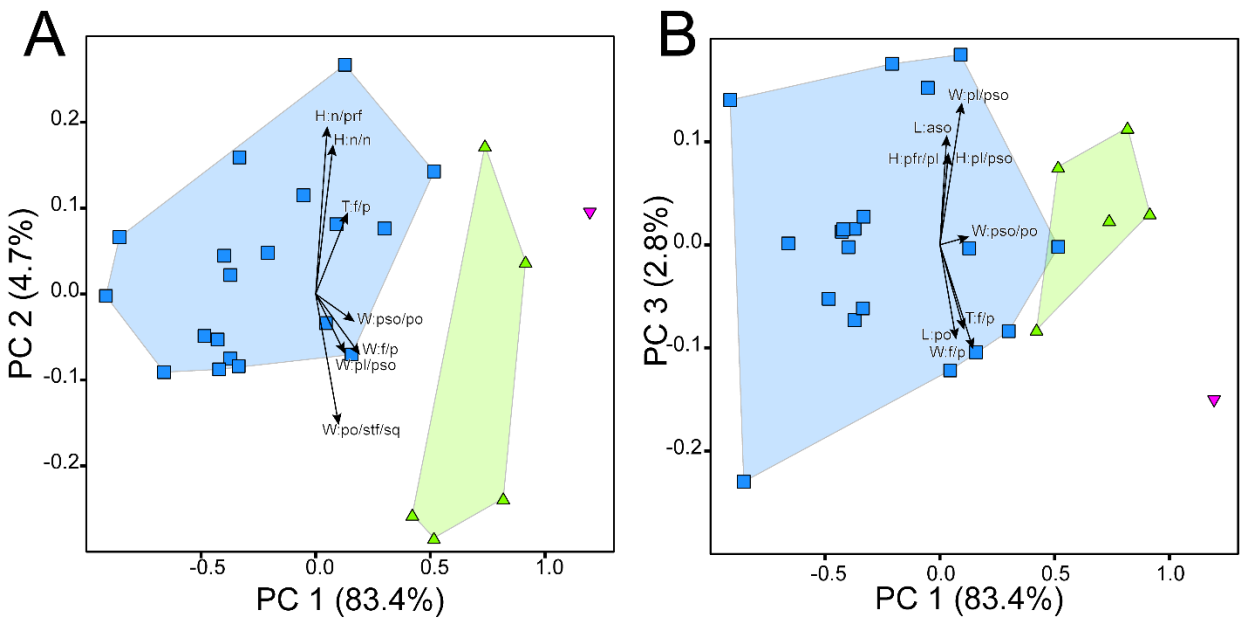

Figure S8. PCA of linear frontoparietal measurements proportionate to the width across the frontoparietal contact TMP 1972.027.0001, *"Hanssuesia sternbergi*, and *Stegoceras validum*. purple inverted triangle – TMP 1972.027.0001; blue squares – *Stegoceras validum*; green triangles – *"Hanssuesia sternbergi*. Arrows indicate eigenvectors of variables; only variables that loaded at least |0.3| in either axis are displayed.

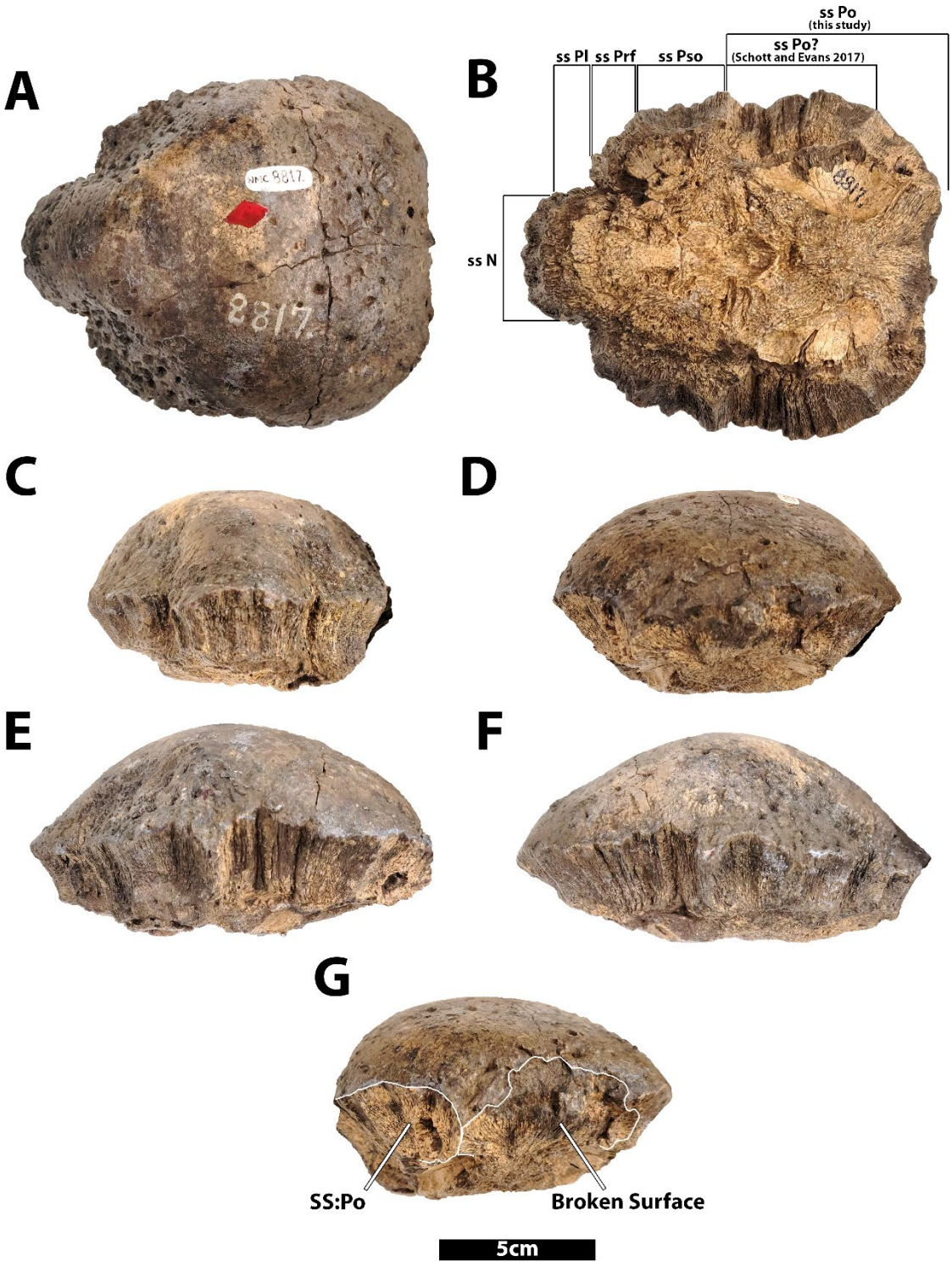

Figure S9. CMN 8817, the holotype specimen of "*Hanssuesia sternbergi*". A) Dorsal. B) Ventral, with peripheral sutural surfaces identified. C) Anterior. D) Posterior. E) Left lateral. F) Right Lateral. G) Posterolateral view of the left temporal region of the parietal. Abbreviations: ss

N, sutural surface for the nasals; ss Pl, sutural surface for the palpebral; ss Po, sutural surface for the postorbital; ss Prf, sutural surface for the prefrontal; ss Pso, sutural surface for the posterior supraorbital.

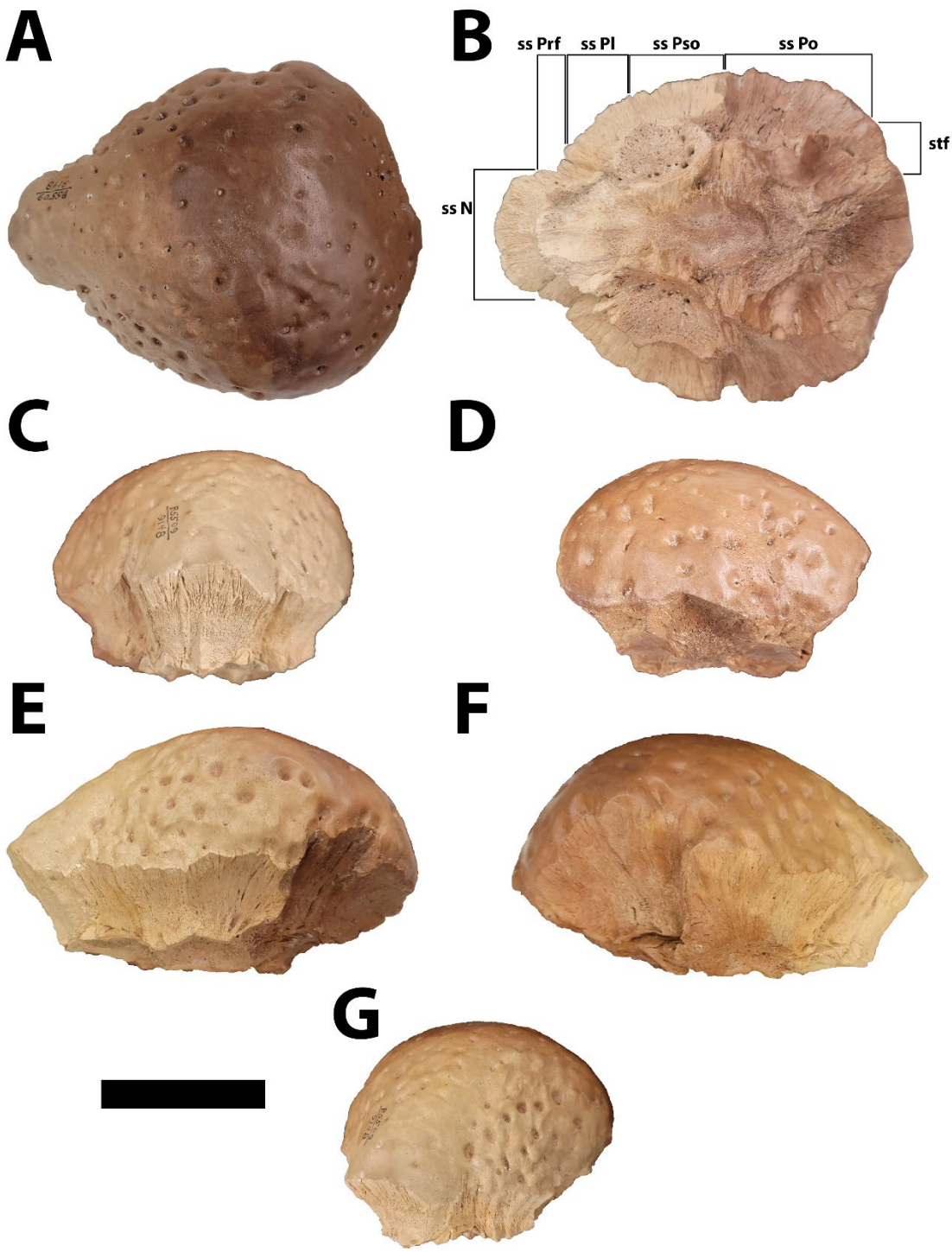

Figure S10. CMN 9148, a pathological frontoparietal of "*Hanssuesia sternbergi*." A) Dorsal, B) ventral, with peripheral sutural surfaces identified. C) Anterior. D) Posterior. Note how the apex of the dome is skewed to the left side. E) Left lateral. F) Right Lateral. G) Anterolateral oblique

view of the left supraorbital region, highlghting pathological pitting and sculpturing of the dorsal surface. Abbreviations: ss N, sutural surface for the nasals; ss Pl, sutural surface for the palpebral; ss Po, sutural surface for the postorbital; ss Prf, sutural surface for the prefrontal; ss Pso, sutural surface for the posterior supraorbital; stf, supratemporal fenestra. Scale bar = 5 cm.

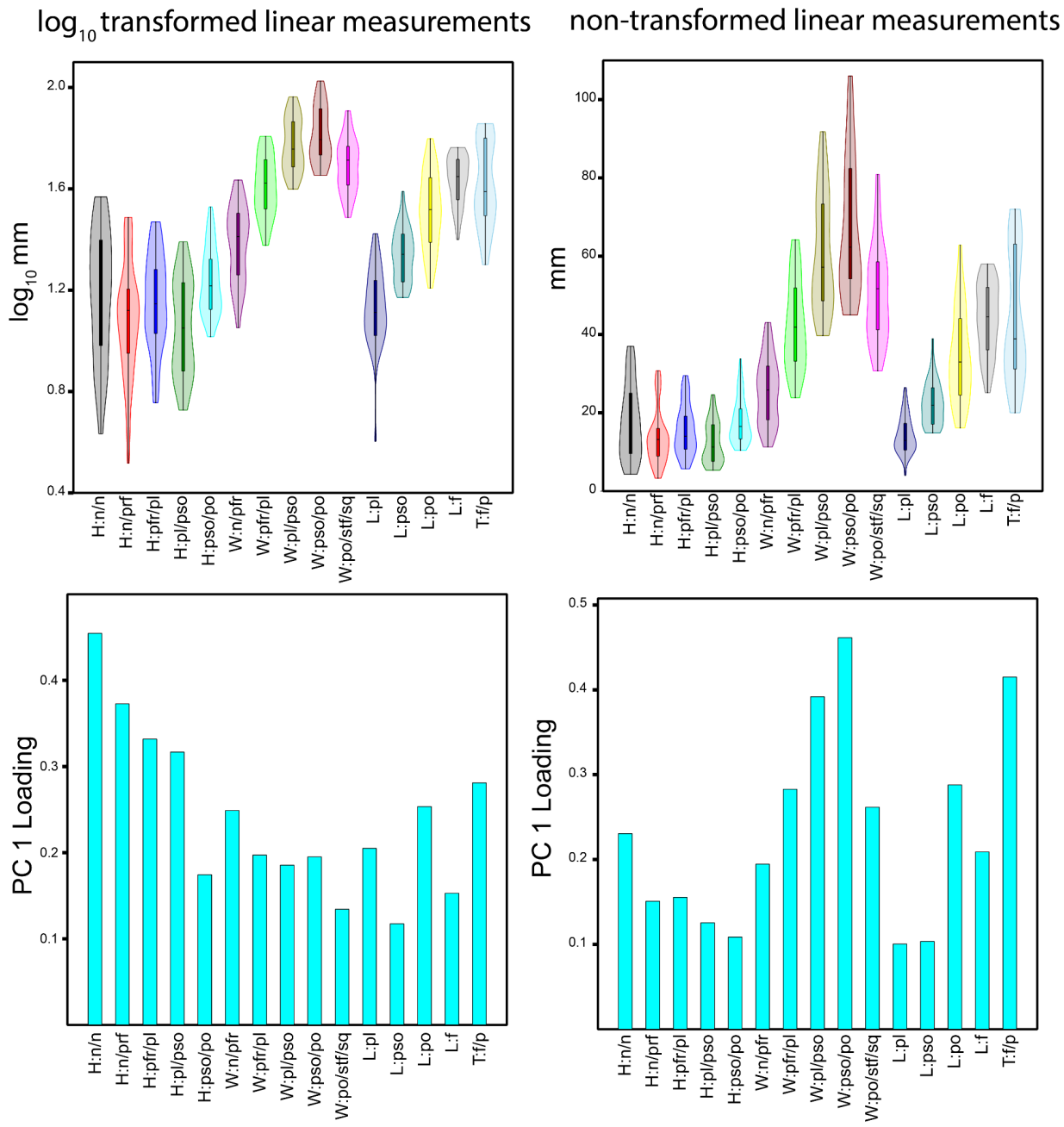

Figure S11. Linear measurement ranges and PC 1 loadings from the Belly River Group PCA. Left column - log_{10}-transformed linear frontoparietal measurements. Right column - non-transformed linear measurements. Log_{10}-transformed has a strong influence on the variables that load PC 1, but does not load PC 1 with measurements that have the absolutely largest ranges.

8. Character Revisions, Character State Revisions, and Taxonomic Reassessments

Woodruff et al. (2021) character (Wch) 7 (character 7 of this analysis). Previously: “Ossified tendons: bundled, rodlike (0); caudal basket, fusiform (1).”

As written, this character represents a problematic character type I-A-4 - Compound state coding (Simões et al., 2017). The condition of “bundled” and “rodlike” define arrangement and morphology, treating them as dependent of one another. It is here rewritten to avoid unjustified dependence and to reflect the analogy (non-homology) between typical ornithischian ossified tendons, and the pachycephalosaurian “caudal basket”. The “caudal basket” is formed by a series of superficial myorhabdoi ossifications (ossified myosepta between caudal myomeres), and are not homologous with the deep paraxial ossified tendon bundles present in other ornithischian clades (Brown and Russell 2012).

Wch 9 (character 9 of this analysis): “Iliac blade, lateral deflection of preacetabular process: weak (0); marked (1).”

We agree with Gilmore (1924), Sues and Galton (1987), and Sereno (2000) that *Stegoceras validum* (UALVP 2) possesses strong lateral deflection in the preacetabular process of the ilium. We reassess *Stegoceras validum* as [1].

Wch 10 (character 10 of this analysis). Previously: “Iliac blade, position of medial tab: absent (0); above acetabulum (1); on postacetabular process (2).”

As written this character represents a problematic character type I-A-2 Absence Coding (Simões et al., 2017). This character was revised to focus on the position of the medial tab (brevis shelf) on the ilium. A new character was created to code for the presence/absence of the medial tab. The absent state [0] of Wch10 was removed to avoid overweighting the condition. Wch 10 state [1] is now state [0]. Wch 10 state [2] is now state [1]. Previous taxonomic assessments follow these changes. *Psittacosaurus mongoliensis* and *Yinlong downsi* are inapplicable for Wch10, as they do not possess a medial tab of the ilium.

Wch 12 (character 12 of this analysis) - Previously: "Ischial pubic peduncle, shape: dorsoventrally (0), or transversely (1); flattened"

This character is rewritten so the "flattening" qualifier is included in both character states, instead of following the state description. Longrich et al. (2010) was correct in assessing *Stegoceras validum* as [0], which we follow here. Sereno (2000) was correct in assessing *Homalocephale calathocercos* and *Prenocephale prenes* as possessing a transversely flattened ischial pubic peduncle [1], and we follow those assessments for these taxa.

Wch 18 (character 18 of this analysis) - Previously: "Supraorbital bones 1 and 2: absent (0); present, and exclude the frontal from the orbital rim (1).

Supraorbitals 1 and 2 are alternative names for the anterior supraorbital and posterior supraorbital (see Sullivan 2003). We interpret the pachycephalosaurian anterior supraorbital as the plesiomorphic ornithischian palpebral (see previous supplementary discussion). Thus, where known, a palpebral is present in all taxa included in this analysis (when enough material is

present to assess the presence of a palpebral, e.g., the sutural surface for the palpebral on the frontal of *Acrotholus audeti*, which is solely known from frontoparietals, Evans et al. 2013). This character is rewritten to focus on the presence of a posterior supraorbital, which appears to be a *de novo* ossification in Pachycephalosauria. We agree with Williamson and Brusatte (2016) and assess *Alaskacephale gangloffi* [?] as the only known specimen is a squamosal (Sullivan 2006).

Wch 19 (character 19 of this analysis) - "Postorbital-jugal bar, position of descending process of postorbital: extends to the ventral margin of the orbit (0); terminates above the ventral margin of the orbit, interdigitate postorbital-jugal contact (1)."

Alaskacephale gangloffi is reassessed as [?], as the only known specimen is a squamosal (Sullivan 2006). Additionally, this character falls into the problematic character Type 1A-7 Unjustified Composite Locator Coding (Simões et al., 2017). The morphology of the ventral margin of the orbit can be made up of one or more skeletal elements. Therefore the reference point of the orbit can be influenced by different elements in different specimens and a single anatomical unit should be specified. This problem was not corrected here, but should be considered in future analyses.

Wch 20 (character 20 of this analysis). Previously: "Parietal septum, form: narrow and smooth (0); broad and rugose, has dorsal ornamentation (1)."

This character is revised to differentiate taxa with a sagittal keel from those with a broad and flattened, often ornate dorsal surface of the parietal in between the supratemporal fenestrae.

Alaskacephale gangloffi is reassessed as [?], as the only known specimen is a squamosal (Sullivan 2006).

Wch 24 (character 24 of this analysis): “Quadratojugal fossa: absent (0); present (1).”

Alaskacephale gangloffi is reassessed as [?], as the only known specimen is a squamosal (Sullivan 2006).

Wch 27 (character 27 of this analysis). Previously: “Epaxial muscle attachment scars on ventrocaudal margin of paroccipital process, caudal view: absent or indistinct (0); broad extending from ventrocaudal margin of paroccipital process and including region above foramen magnum (1); restricted to area dorsolateral to foramen magnum (2).”

Tsuihiji (2010) identified these “epaxial muscle attachments” as the insertion area for the atlanto-occipital capsular membrane/ligament. Although Tsuihiji’s (2010) interpretation of the insertion area for the atlanto-occipital capsular membrane ligament encircles the occipital condyle and foramen magnum, it includes the large depressions described by Wch 27. The character is revised to specify this membrane. The “absent or indistinct” state was removed, as all taxa with suitable preservation preserve at least a shallow depression. Character state revised to: positioned lateral to the foramen magnum [0] (previously state 1); positioned dorsal to the foramen magnum [1] (previously state 2). *Homalocephale calathocercos* (MPC-D 100/1201; Tsuihiji 2010)*, Psittacosaurus mongoliensis* (IGM 100/1032, fig 6 in Tsuihiji 2010)*, Sphaerotholus buchholtzae* (DMNH EPV.97077), and *Yinlong downsi* (fig 20 in Han et al. 2016)

are reassigned as [0]. *Pachycephalosaurus wyomingensis* (UALVP 444, a cast of AMNH 1696) is reassigned as [1].

A rendered 3D model of DMNH EPV.97077 was accessed from http://n2t.net/ark:/87602/m4/M18280. The Witmer Lab at Ohio University provided access to these data (frontoparietal) originally appearing in The Visible Interactive Pachycephalosaur, the collection of which was funded by NSF grants to LM Witmer. The files were downloaded from www.MorphoSource.org, Duke University

Wch 28 (character 28 of this analysis). Previously: "Supratemporal fenestra: open (0); closed (1)"

This character is revised to specify the condition of the supratemporal fenestrae at maturity. The supratemporal fenestrae of *Foraminacephale brevis* (Schott and Evans 2017) and *Pachycephalosaurus wyomingensis* (Horner and Goodwin 2009) close through ontogeny. They remain open throughout ontogeny in *Colepiocephale lambei* (Schott et al. 2009), and are occasionally closed in *Stegoceras validum* without any relationship to ontogeny (Schott and Evans 2012). All other pachycephalosaurid taxa known from mature material do not possess open temporal fenestrae. Character state [0] is revised to specify that the supratemporal fenestrae remain open throughout ontogeny. *Colepiocephale lambei* re-assigned as [0] (Schott et al. 2009). *Goyocephale lattimorei*, *Homalocephale calathocercos*, and *Wannanosaurus yansiensis* are re-assigned [?] due to the immature status of the only known specimens (Butler and Zhao 2009; Evans et al. 2011).

Wch 29 (character 29 of this analysis). Previously: “Roof of temporal chamber as manifest on parietal in lateral view: absent (0); small, roof horizontal (1); enlarged, dorsally arched (2)”

This character as was written, represents a problematic Type IA-5 character - Compound State-coding (Simões et al., 2017). A small and temporal chamber is united with the orientation of the roof, or a dorsal arch with a large chamber, without clear biological dependence. This character was originally created by Williamson and Carr (2002) (character 41 of their analysis). Williamson and Carr (2002) only assessed the inclination of the temporal roof, and did not include a size aspect to the character states. Wch29 was revised back to Williamson and Carr’s (2002) initial wording. This character is difficult to assess without a horizontal plane of reference. For example, NMMNH P-27403 (*Sphaerotholus goodwini*) has been historically figured with the posterovental margin of the parietal positioned above the anteroventral margin of the frontal at an angle of ~16° (fig 1 in Williamson and Carr 2002). This exaggerates the inclination of the temporal roof, and appears extremely posterodorsal inclined. When the specimen is rotated such that the posteroventral margin of the parietal is horizontal with the anterovenral margin of the frontal, the posterodorsal inclination of the temporal roof is far less extreme. Dichotomization of states for this character would greatly benefit from a quantitative analysis. *Wannanosaurus yansiensis* is tentatively reassigned (0). *Amtocephale gobiensis* and *Sphaerotholus goodwini* are tentatively reassigned (1). *Acrotholus audeti* and *Colepiocephale lambei* are tentatively assigned (2) (Schott et al. 2009 described the temporal roof of *Colepiocephale lambei* as posterodorsally inclined). *Alaskacephale* and *Sinocephale bexelli* are tentatively resigned (?), due to the difficulty of orienting these fragmentary specimens.

Wch30 (character 30 of this analysis) – “Grooves in frontal: absent (0); present (1)”

This character is revised to reflect the development of the groove on the frontal portion of the dome. Taxa that were previously assessed as "present" develop these grooves during dome inflation. Uninflated juveniles of these taxa (e.g., *Foraminacephale brevis*, *Stegoceras validum*) do not possess grooved frontals. The character is also revised to specify the position of the groove, which separates the frontonasal boss from the supraorbital lobes. *Tylocephale gilmorei* is reassessed as (?) as the entire dorsal surface of the frontals are damaged (Maryańska and Osmólska 1974). *Goyocephale lattimorei* and *Homalocephale calathocercos* are reassigned as (?) due to the juvenile, uninflated nature of the only known specimens (Evans et al. 2011). Williamson and Brusatte (2016) were correct to reassess *Alaskacephale gangloffi* as (?), as the sole known specimen is a squamosal and does not preserve a frontal.

Wch 31 (character 31 of this analysis). Previously: "Contact of anterior supraorbital with frontal: absent (0); restricted (1); extensive (2)."

"Anterior supraorbital" is corrected to palpebral (see previous discussion). This character represents a problematic character Type IIB - Continuous data unjustifiably treated as discrete (Simões et al., 2017). The delineation between "restricted" or "extensive" is arbitrary without some reference point or disjoint ranges of its proportional development. Dichotomization of "restricted" vs. "extensive" would greatly benefit from a quantitative analysis. *Sphaerotholus edmontonensis* and *Sphaerotholus goodwini* are reassessed as (2), as the frontal-palpebral contact of the holotype specimens are more comparable to similarly sized specimens of *Stegoceras validum* than to specimens of *Sphaerotholus buchholtzae* or *Prenocephale prenes*. *Acrotholus audeti* was reassessed as (1/2), as the paratype specimen (ROM 2964) has a proportionally broad frontal-palpebral contact. See Table S24 for measurements.

Wch 32 (character 32 of this analysis). “Doming of frontoparietal: absent (0); does not include supraorbital lobes (1); includes supraorbital lobes (2)”

Goyocephale lattimorei, *Homalocephale calathocercos*, and *Wannanosaurus yansiensis* are re-assigned [?] due to the immature status of the only known specimens (Butler and Zhao 2009; Evans et al. 2011).

Wch 33 (character 33 of this analysis): Previously: “Dorsal margins of postorbital and posterior supraorbital sutural surfaces on dome: postorbital and supraorbital II do not form part of a dome (0); dorsally arched such that there is a distinct diastema between the two (1); both are straight and continuous, diastema absent (2).”

The [0] character (describing exclusion from the dome) was removed as the posterior supraorbital and postorbital are incorporated into the dome through ontogeny. All pachycephalosaurians previously assessed with this character are solely known from juvenile remains. *Goyocephale lattimorei*, *Homalocephale calathocercos*, and *Wannanosaurus yansiensis* are re-assigned [?] due to the immature status of the only known specimens (Butler and Zhao 2009; Evans et al. 2011). *Psittacosaurus mongoliensis* and *Yinlong downsi* are reassessed as inapplicable, as they do not possess a posterior supraorbital or a frontoparietal dome.

Wch34 (character 34 of this analysis). Previously: “Frontoparietal dome in lateral view, caudal margin of parietal dome blends with parietosquamosal shelf along a curve: absent (0); present (1)”

This character is revised to discuss the extent that the parietal is incorporated into the cranial dome. *Goyocephale lattimorei*, *Homalocephale calathocercos*, and *Wannanosaurus yansiensis* are re-assigned [?] due to the immature status of the only known specimens (Butler and Zhao 2009; Evans et al. 2011). *Stegoceras validum* is re-assessed as (0/1).

Wch35 (character 35 of this analysis): Previously: “Parietosquamosal bar in caudal view (viewed perpendicular to shelf): horizontal or slopes at a shallow ventrolateral angle (0); slopes at a steep ventrolateral angle (1).

This character represents a problematic character type IIB - Continuous variable unjustifiably treated as discrete (Simões et al., 2017). The difference between “shallow” and “steep” is unclear without demonstration of a disjunct range in angles, one being distinctly shallow compared to the other. We’ve revised this character to focus on the squamosal, as the parietal portion of the parietosquamosal bar is always horizontal. Specifically, we focus on the posterior ventral margin of the squamosals. *Alaskacephale gangloffi* is reassessed as [0], assuming the posterior most contact of the squamosal with the parietal is vertical. *Foraminacephale brevis*, *Pachycephalosaurus wyomingensis*, and *Prenocephale prenes* are reassessed as [1]. Distinguishing between these character states would greatly benefit from quantitative analyses.

Wch 36 (character 36 of this analysis). Previously: “Parietosquamosal bar beneath the primary node row: absent (0); maintains approximately the same depth or slightly deepens laterally (1); shallows laterally (2).

This character represents a problematic character type IIB - Continuous variation arbitrarily treated as discrete (Simões et al., 2017). The difference between deepening and shallowing of the posterior squamosal bar should be quantified to demonstrate how much, if any, disjunct there is between these proposed states. Woodruff et al. (2021) reported that this character is variable in *Sphaerotholus buchholtzae* (ROM 75853 does not laterally decline). We find that the reported lateral shallowing of the region below the primary node row does not significantly differ from specimens that maintain a constant depth mediolaterally across the posterior squamosal margin. Instead, we suggest that squamosals of *Stegoceras validum* are uniquely laterally deep, and are more distinct from a constant depth along the mediolateral vector, than are purported squamosals that shallow laterally. Character state [1] is revised to include morphologies that are approximately the same depth, or slightly shallow laterally. Character state [2] is revised to include morphologies that greatly deepen laterally. Distinction between character states would greatly benefit from quantitative analyses. *Sphaerotholus buchholtzae* and *Sphaerotholus goodwini* are reassessed as [1]. *Stegoceras validum* is reassessed as [2]. *Homalocephale calathocercos*, *Goyocephale lattimorei*, and *Wannanosaurus yansiensis* are reassessed as ? due to the immaturity of the specimens, and the ontogenetic deepening of the bar in *Stegoceras validum*.

Wch 37 (character 37 of this analysis) - was “Exposure of posteromedian (intersquamosal) process of the parietal between squamosals: caudolateral wings well developed (0); restricted (1); broad (2).”

This character represents a problematic character type IIB - Continuous variation arbitrary treated as discrete (Simões et al., 2017). The delineation between “broad” and “restricted” should be demonstrated with clear disjunct, otherwise treated as continuous. We did not perform this task here, but we have revised the character following our own observations and interpretations. The “broad” and “restricted” states are switched so the series from 0, 1, and 2 reflects a continuous decrease in the posterior exposure of the parietal. The “restricted” state [2] is revised to include absence of posterior parietal exposure (formed by intersquamosal contact). This is the logical continuation of reduced posterior parietal exposure and when is only ever polymorphic for a taxon when multiple specimens are known (*Stegoceras validum*; *Pachycephalosaurus wyomingensis,* intersquamosal contact in some “*Stygimoloch spinifer*” ontogimorphs (e.g. MPM 8111), but not others (e.g. MPM 7111) Sullivan 2003). *Foraminacephale brevis, Goyocephale lattimorei*, *Homalocephale calathocercos*, *Sphaerotholus buchholtzae*, and *Sphaerotholus edmontonensis* are reassigned [1]. *Acrotholus audeti*, *Amtocephale gobiensis, Sinocephale bexelli*, and *Sphaerotholus goodwini* are reassessed as [2], *Pachycephalosaurus wyomingensis* is reassessed as [1/2] (broad in AMNH 1696; restricted in MPM 7111, intersquamosal contact in MPM 8111) *Stegoceras validum* are reassessed as [1/2] (broad in TMP 1972.027.0001, restricted in UALVP 2, intersquamosal contact in CMN 8816). This distinction between character states would greatly benefit from quantitative analyses.

Wch 38 (combined with Wch 37, character 37 of this analysis). Previously: “Extensive intersquamosal joint posterior to parietal: absent (0), present (1).”

Caudolateral wings, “broad” posterior medial extension, “restricted” posterior medial extension, and intersquamosal contact form a transitional series. Thus Wch 37 and 38 are problematic character type IA2, which splits states of single transformational series (Simões et al. 2017)

Wch 39 (character 38 of this analysis) – was “Parietosquamosal bar primary (enlarged) nodes: absent (0); in a single row (1); in two or more rows sometimes appearing clustered (2).”

Character state 2 was removed, and a new character was created to assess the presence/ absence of enlarged nodes dorsal to the primary node row (character 49 of this analysis). *Pachycephalosaurus wyomingensis* is reassessed as [1]. Nodes 1 and 4 of Horner and Goodwin (2009) are interpreted as the primary node row, whereas nodes 2 and 3 are interpreted as ventrolateral corner nodes.

Wch 40 (removed for this analysis) – “Number of nodes in the primary parietosquamosal node row: 5 or less (0) 6 or more (1)”

This character fails the primary homology test of conjunction (Patterson 1982, de Pinna 1991; problematic character type ID of Simões et al. 2017), and was therefore removed from the character matrix. Both character states are present in MPC-D 100/51 (*Goyocephale lattimorei*) and likely present in ROM 75835 (*Sphaerotholus buchholtzae*). MPC-D 100/51 preserves five

primary nodes on the left side, and seven on the right. Woodruff et al. (2021) reported that ROM 75835 possessed five primary nodes, and that the medial most node was almost entirely positioned on the parietal. We interpret four preserved nodes on the right side, with the right medial most node almost entirely positioned on the squamosal, and the fifth, corner (vertex) node damaged and absent. The left side preserves six primary nodes, with the medial most positioned almost entirely on the parietal, and the lateral most two damaged, but still preserve the rounded outlines of their bases.

Wch 41 (character 39 of this analysis) - was "Irregular tuberculate ornamentation on caudal surface of squamosal below the primary node row: absent (0); present (1)."

This character is revised to reflect the probable homology between the "minute tubercles" and "posterior accessory nodes", with the major difference being the arrangement and distribution of these minute nodes. State [1] is revised to reflect taxa which only possess minute nodes immediately ventrally adjacent to the primary node row, with the remaining (ventral most) posterior surface of the squamosal being smooth. State [2] is created to reflect taxa that have extensive minute nodes, which cover the entire posterior surface of the squamosal. *Alaskacephale gangloffi*, *Prenocephale prenes*, *Sphaerotholus goodwini*, and *Yinlong downsi* are all assessed as [0]. *Foraminacephale brevis* is assessed as [1] (Schott and Evans 2017). *Sphaerotholus buchholtzae* is assessed as [1]. *Goyocephale lattimorei*, *Homalocephale calathocercos*, *Stegoceras validum*, and *Tylocephale gilmorei* are reassessed as [2]. *Wannanosaurus yansiensis* is reassessed as [?] due to the damaged posterior surface of the

holotype's squamosal (Butler and Zhao 2009). *Pachycephalosaurus wyomingensis* is assessed as inapplicable, as the posterior surface of the squamosals are entirely covered in large nodes. *Psittacosaurus mongoliensis* is reassessed as inapplicable.

Wch 42 (not included in this analysis) – "A coalescing node with constituents on the parietal and squamosal (i.e. a parietosquamosal node): absent (0); present (1)"

This character in previous studies described the medial most node of the primary parietosquamosal node row (e.g., Evans et al. 2013). This character is problematic (Type IA Simões et al. 2017), as it may not be independent from the exposure of the intersquamosal process of the parietal (Wch 37 and 38), whereby wider intersquamosal processes of the parietal are likely to contact the medialmost node of the primary node row. Indeed, character assessments for Wch 37 and Wch 42 were completely congruent, aside from *Stegoceras validum* (which is polymorphic), "*Stegoceras novomexicanum*" (which we follow Williamson and Brusatte 2016 as regarding *nomen dubium*), and *Sinocephale bexelli* (though the presence of a primary squamosal node row is unknown, and would therefore be inapplicable for this character) and (problematic character type I B). Additionally, the character states fail the primary homology test of conjunction (Patterson 1982, de Pinna 1991) in TMP 2017.012.0019, which possesses a coalescing node on the right side but not the left (Fig. S2).

Variation in the sagittal space between the left and right primary node rows has not been assessed, but may also vary independent of the parietal-squamosal contact. Future studies should examine the relationship and possible independence of the breadth of the posterior parietal

exposure and distance between the primary node rows, which may be phylogenetically informative.

Wch 43 (character 40 of this analysis) – Previously: “Medialmost nodes in primary parietosquamosal node row, enlarged relative to all other nodes: absent (0); present (1).”

This character represents a problematic character type IIB - Continuous variation treated as discrete (Simões et al., 2017). Taken word for word, any degree larger the medialmost nodes would be considered “enlarged”. A clear distribution with disjunct between ranges would be needed to justify its use as a discrete character. This was not performed in this study. Instead, we reassessed the specimens and reinterpreted which ones displayed a more clearly enlarged medialmost node. *Alaskacephale gangloffi* is reassigned as [1] (Gangloff et al. 2005). *Psittacosaurus mongoliensis* and *Yinlong downsi* are reassigned as inapplicable. *Sphaerotholus buchholtzae* is reassigned as [0/1] (TMP1987.113.0001 is [0], DMNH EPV.97077 is [1]; Woodruff et al. 2021). *Pachycephalosaurus wyomingensis* is reassigned as [0/1].

Wch 44 (character 41 of this analysis). – “Enlarged corner node on squamosal ventrolateral to primary node row of parietosquamosal bar: absent (0); present (1).”

This character represents a problematic character type IIB - Continuous variation treated as discrete (Simões et al., 2017). Taken word for word, any degree larger the corner nodes would be considered “enlarged”. A clear distribution with disjunct between ranges would be needed to justify its use as a discrete character. This was not performed in this study. Instead, we reassessed the specimens and reinterpreted which ones displayed a more clearly enlarged corner

node. These observations apply to the next character referring to corner nodes as well. *Psittacosaurus mongoliensis* is reassessed as inapplicable as it does not possess a primary node row.

Wch 45 (character 42 of this analysis). Previously: “Secondary corner node, medial to the lateroventral corner node: absent (0); present (1).”

“Enlarged corner nodes” are herein described as the ventral node row (ventral to the primary node row). These character states are revised to reflect the number of nodes in the ventral node row. Previous scoring suggested that not possessing multiple ventral nodes (primary and secondary corner node) (e.g., *Prenocephale prenes*) was homologous with not possessing any ventral nodes (e.g., *Stegoceras validum*). An absence character state was not added, as it is already addressed in Wch 44 (revised to reflect the presence or absence of enlarged nodes ventral to the primary node row). *Pachycephalosaurus wyomingensis* is reassessed as [1] *Alaskacephale gangloffi* is reassessed as [?], as we cannot discern if the second node row represents a dorsal node row or a ventral node row. *Psittacosaurus mongoliensis, Stegoceras validum*, *Yinlong downsi,* and *Wannanosaurus yansiensis* reassessed as inapplicable, as they do not possess any enlarged nodes ventral to the primary node row.

Wch 48 (character 45 of this analysis) - “Rostral nodes: absent (0); continue from the supraorbital shelf onto the dorsal region of the rostrum (1); cover the dorsal surface of rostrum and form series of ‘half rings’ (2).”

This character was revised to specify the arrangement of rostral nodes. The absence character was removed to avoid double scoring (overweighting) this state with a new character (character 48 of this analysis), which addresses the presence/absence of rostral ornamentation. *Stegoceras validum*, *Psittacosaurus mongoliensis*, and *Yinlong downsi* were reassessed as inapplicable, as they do not possess any rostral ornamentation.

Wch 49 (character 46 of this analysis) – "Postorbital node row: absent (0); present (1)"

This character is revised to describe the dorsolateral ridge of the postorbital. State [0] is revised to unite dorsolateral ridge with a series of reduced rectangular nodes. State [1] is revised to describe enlarged, circular nodes. *Goyocephale lattimorei* and *Homalocephale calathocercos* are reassessed as [0]. *Sphaerotholus goodwini* and *Tylocephale gilmorei* are reassessed as [1]. *Psittacosaurus mongoliensis* was reassessed as inapplicable.

Wch 50 (character 47 of this analysis) – "Posterolateral edge of skull formed by squamosal and postorbital in dorsal view: straight (0); convex (1).

Sphaerotholus buchholtzae and *Sphaerotholus goodwini* are reassessed as [0] based on DMNH EPV.97077 (Woodruff et al. 2021) and NMMNH P-27403 (Williamson and Carr 2002) respectively. *Foraminacephale brevis* and *Sphaerotholus edmontonensis* are reassessed as [?], due to the lack of complete or known, articulated postorbitals and squamosals. Schott and Evans (2017) described articulated postorbitals and squamosals in ?TMP 1970.010.0002 (*Foraminacephale brevis*), although the lateral outlines of these elements are damaged.

Wch 51 (not included in this analysis) - “Posterior accessory node on squamosal ventral to nodes 3 and 4 in the primary parietosquamosal node row: absent (0); present (1).

“Posterior accessory nodes” are herein considered homologous with the “minute tubercles” described on the posterior walls of other pachycephalosaurid squamosals (e.g., *Stegoceras validum*). We find the main difference between these purported terms to be their arrangement and distribution across the squamosal. “Posterior accessory nodes” are formed when this ornamentation is restricted immediately ventral to the primary node row. “Minute nodes” (or “irregular tuberculate ornamentation”) are more disorganised, and cover the entire posterior surface of the squamosal. Wch 41 (character 39 of this analysis) was revised to describe the distribution of these smaller, posterior nodes across the posterior surface of the squamosal.

New Characters

Character 48: Enlarged rostral: absent (0), present (1). (new)

This character codes for the presence/absence of rostral ornamentation. Wch 48 coded for differences in the arrangement of rostral ornamentation, but did not unite pachycephalosaurians that possessed rostral ornamentation. *Psittacosaurus mongoliensis*, *Stegoceras validum*, and *Yinlong downsi* are assessed as [0]. *Goyocephale lattimorei*, *Pachycephalosaurus wyomingensis*, and *Prenocephale prenes* are assessed as [1]. All other taxa are assessed as [?].

Character 49: Enlarged nodes dorsally adjacent to the primary parietosquamosal node row: absent (0); present (1).

We reject the primary homology assessment of two dorsal node rows and nodes appearing as a cluster (Wch 39 [2]). Instead, we propose that the "clustered" appearance of some *Pachycephalosaurus wyomingensis* specimens represents a modified primary node row, ventrolateral corner nodes, and dorsal node row. Characters 41 and 42 of this analysis code for the presence/absence and number of lateroventral corner nodes respectively. State [0] of character 49 (new) codes for the absence of enlarged nodes along the posterodorsal margin of the squamosal. State [1] codes for the presence of enlarged nodes dorsal to the primary node row. *Foraminacephale brevis*, *Homalocephale calathocercos*, *Prenocephale prenes, Psittacosaurus mongoliensis, Sphaerotholus buchholtzae*, *Sphaerotholus goodwini*, *Stegoceras validum* and *Yinlong downsi* are assessed as [0]. *Alaskacephale gangloffi*, *Goyocephale lattimorei*, and *Pachycephalosaurus wyomingensis* are assessed as [1]. All other taxa are assessed as [?].

Character 50 – Medial tab (brevis shelf) of ilium: absent [0]; present [1].

This character was created to unite taxa that possessed a medial tab of the ilium.

Character 51: Parietal septum in between supratemporal fenestrae (prior to incorporation into frontoparietal dome): narrow [0]; broad [1]

This character is only applicable to taxa that are represented by juvenile remains, prior to the entire parietal being incorporated into the dome. *Goyocephale lattimorei* and

Pachycephalosaurus wyomingensis are assessed as [0]. *Foraminacephale brevis*, *Homalocephale calathocercos*, and *Stegoceras validum* are assessed as [1]. Although Schott et al. (2009) interpreted a narrow parietal septum between the supratemporal fenestrae of *Colepiocephale lambei*, it is currently unknown if that narrow extension formed a sagittal keel, or a flattened, dorsally ornate surface, and so it is assessed as [?]. To avoid overweighting the presence of a sagittal keel, *Psittacosaurus mongoliensis* and *Yinlong downsi* are inapplicable for this character. All other taxa are assessed as [?]. This character as constructed represents a problematic character type IIB - Continuous variation unjustly treated as discrete (Simões et al., 2017). Although we interpret a clear distinction between "narrow" and "broad" quantification of this will need to be undertaken for the continued use of this character.

Character 52: Dorsolateral edge of the skull in dorsal view along the posterior supraorbital - postorbital contact: straight [0]; medial indentation [1].

Homalocephale calathocercos, *Pachycephalosaurus wyomingensis*, *Sphaerotholus buchholtzae*, *Sphaerotholus goodwini*, *Tylocephale gilmorei*, and *Wannanosaurus yansiensis* are assessed as [0]. *Goyocephale lattimorei* and *Prenocephale prenes* are assessed as [1]. *Psittacosaurus mongoliensis* and *Yinlong downsi* are assessed as inapplicable due to the absence of a posterior supraorbital. All other taxa are assessed as [?].

9. Phylogenetic Characters and Character States used in this Study

1. Posterior sacral rib length: short and subrectangular (0); strap-shaped and elongate (1) - character 1 of Woodruff et al. (2021).
2. Preacetabular process, shape of distal end: tapered and subveritcally oriented (0); dorsoventrally flattened and expanded distally (1) - character 2 of Woodruff et al. (2021).
3. Humeral length: more (0), or less than (1), 50% of femoral length - character 3 of Woodruff et al. (2021).
4. Humeral shaft form: straight (0); bowed (1); rudimentary (1) - character 4 of Woodruff et al. (2021).
5. Deltopectoral crest development: strong (0); rudimentary (1) - character 5 of Woodruff et al. (2021).
6. Zygapophyseal articulations, form: flat (0); grooved (1) - character 6 of Woodruff et al. (2021).
7. Caudal myorhabdoi ossifications: absent (0); present (1) - character 7 (revised) of Woodruff et al. (2021).
8. Sternal shape: plate-shaped (0); shafted (1) - character 8 of Woodruff et al. (2021).
9. Iliac blade, lateral deflection of preacetabular process weak (0); marked (1) - character 9 of Woodruff et al. (2021).
10. Iliac blade, position of medial tab: dorsal to acetabulum (0); on post acetabular process (1).- character 10 (modified) of Woodruff et al. (2021).
11. Postacetabular process of ilium: elongate and subrectangular (0); deep and downturned distally, with an arcuate dorsal margin (1) - character 11 of Woodruff et al. (2021).

12. Ischial pubic peduncle, shape: dorsoventrally flattened (0), transversely flattened (1) - character 12 (modified) of Woodruff et al. (2021).
13. Pubic body: substantial (0); reduced, nearly excluded from acetabulum (1) - character 13 of Woodruff et al. (2021).
14. Frontal and parietal thickness: thin (0); thick (1) - character 14 of Woodruff et al. (2021).
15. Arched premaxilla-maxilla diastema: absent (0); present (1) - character 15 of Woodruff et al. (2021).
16. Postorbital-squamosal bar, form: strap-shaped with a narrow dorsal margin (0); broad, flattened (1) - character 16 of Woodruff et al. (2021)
17. Squamosal exposure on occiput: restricted (0); broad (1) - character 17 of Woodruff et al. (2021).
18. Posterior supraorbital: absent (0), present, participates with palpebral in excluding the frontal from the orbital rim (1) - character 18 (modified) of Woodruff et al. (2021).
19. Postorbital-jugal bar, position of descending process of postorbital: extends to the ventral margin of the orbit (0); terminates above the ventral margin of the orbit, interdigitate postorbital-jugal contact (1) - character 19 of Woodruff et al. (2021).
20. Parietal between supratemporal fenestrae: forms a sagittal keel (0), formed by a dorsally flattened ornate surface (1) - character 20 (modified) of Woodruff et al. (2021).
21. Infratemporal fenestra size: larger than orbit, lower temporal bar long (0); smaller than orbit, lower temporal bar greatly shortened, jugal and quadrate in close proximity or have a small contact (1) - character 21 of of Woodruff et al. (2021).

22. Pterygoquadrate rami, posterior projection of ventral margin: weak, jaw joint at the approximate level of occlusal surface (0); pronounced, jaw joint below occlusal surface (1) - character 22 of Woodruff et al. (2021).
23. Prootic-basisphenoid plate: absent (0); present (1) - character 23 of Woodruff et al. (2021).
24. Quadratojugal fossa: absent (0); present (1) - character 24 of Woodruff et al. (2021).
25. Quadrate, posterior ramus in lateral view: subvertical or gently curved dorsally (0); sinuous, quadrate strongly inclined dorsally, posterior ramus embayed (1) - character 25 of Woodruff et al. (2021).
26. Skull: relatively short, rostrum has a convex profile (0); relatively long, rostrum has a concave dorsal profile (1) - character 26 of Woodruff et al. (2021).
27. Position of the major bilateral depressed insertion area for the atlanto-occipital capsular membrane/ligament: lateral to the foramen magnum (0); dorsal to the foramen magnum (1) - character 27 (modified) of Woodruff et al. (2021).
28. Supratemporal fenestra: remain open throughout ontogeny (0); closed (1) - character 28 (modified) of Woodruff et al. (2021).
29. Roof of temporal chamber as manifest on parietal in lateral view: absent (0); sub-horizontal (1); posterodorsally inclined (2) - character 29 (modified) of Woodruff et al. (2021).
30. Grooves separating frontonasal boss from supraorbital lobes on frontal: absent (0); present (1) - character 30 (modified) of Woodruff et al. (2021).
31. Contact of palpebral with frontal: absent (0); restricted (1); extensive (2) - character 31 (modified) of Woodruff et al. (2021).

32. Doming of frontoparietal: absent (0); does not include supraorbital lobes (1); includes supraorbital lobes (2) - character 32 of Woodruff et al. (2021).
33. Dorsal margins of postorbital and posterior supraorbital sutural surfaces on dome: dorsally arched such that there is a distinct diastema between the two (0); both are straight and continuous, diastema absent (1) - character 33 of Woodruff et al. (2021).
34. Parietal portion of cranial dome: extends to posterior margin of the parietal, forming a "down-turned" parietal (0); does not extend to posterior margin, but forms a posterior parietal shelf (1) - character 34 (modified) of Woodruff et al. (2021).
35. Mediolateral orientation of the ventral margin of the squamosal in posterior view: horizontal or slopes at a shallow ventrolateral angle (0); slopes at a steep ventrolateral angle (1) - character 35 (modified) of Woodruff et al. (2021).
36. Parietosquamosal bar beneath the primary node row: absent (0); maintains approximately the same depth or slightly shallows (1); deepens laterally (2). - character 36 (modified) of Woodruff et al. (2021).
37. Exposure of posteromedian (intersquamosal) process between squamosals: caudolateral wings well developed (0); broad (1); restricted or absent (2) - characters 37 and 38 (modified) of Woodruff et al. (2021).
38. Primary (enlarged) nodes (node row) along posterodorsal margin of squamosals: absent (0); present (1) - character 39 (modified) of Woodruff et al. (2021).
39. Ornamentation consisting of minute tubercles ventral to the primary node row: absent (0); adjacent to primary node row, with an unornamented ventral region (1), extensive over the posterior wall (2) - characters 41 and 51 (modified) of Woodruff et al. (2021).

40. Size of medialmost nodes in primary parietosquamosal node row relative to successive lateral nodes: subequal (0); enlarged (1) - character 43 (modified) of Woodruff et al. (2021).
41. Enlarged corner node on squamosal ventrolateral to primary node row of parietosquamosal bar: absent (0); present (1) - character 44 of Woodruff et al. (2021).
42. Number of enlarged ventrolateral corner nodes: single corner node (0); at least two corner nodes (1) - character 45 (modified) of Woodruff et al. (2021).
43. Squamosal, several nodes drawn out into long spikes: absent (0); present (1) - character 46 of Woodruff et al. (2021).
44. Large, conical node projects laterally from jugal: absent (0); present (1). character 47 of Woodruff et al. (2021).
45. Arrangement of rostral nodes: continue from the supraorbital shelf onto the dorsal region of the rostrum (0); cover the dorsal surface of rostrum and form a series of 'half rings' (1) - character 48 (modified) of Woodruff et al. (2021).
46. Ornamentation along the dorsolateral ridge of postorbital: a low ridge or series of low, rectangular nodes (0); row of enlarged circular nodes (1) - character 49 (modified) of Woodruff et al. (2021).
47. Posterolateral edge of skull formed by squamosal and postorbital in dorsal view: straight (0); convex (1) - character 50 of Woodruff et al. (2021).
48. Nasal ornamentation: absent (0): present (1). (new)
49. Enlarged ornamentation on the dorsal surface of the squamosal: absent (0), present (1). (new)
50. Medial tab of ilium: absent (0); present (1). (new)

51. Parietal septum in between supratemporal fenestrae (before closure): narrow [0], broad [1]. (new)
52. Diastema between posterior supraorbital and postorbital on dorsolateral ridge (dorsal view): absent (0), present (1). (new)

10. Supplementary References

Brown, B. and E.M. Schlaikjer. 1943. A study of the troödont dinosaurs with the description of a new genus and four new species. Bulletin of the American Museum of Natural History 82:115–150.

Brown, C.M. and A.P. Russell. 2012. Homology and architecture of the caudal basket of Pachycephalosauria (Dinosauria: Ornithischia): The first occurrence of myorhabdoi in Tetrapoda. PLoS ONE 7:e30212.

Butler, R.J. and Q. Zhao. 2009. The small-bodied ornithischian dinosaurs *Micropachycephalosaurus hongtuyanensis* and *Wannanosaurus yansiensis* from the Late Cretaceous of China. Cretaceous Research 30:63–77.

Dieudonné P.-E., P. Cruzado-Caballero, P. Godefroit and T. Tortosa. 2020. A new phylogeny of cerapodan dinosaurs. Historical Biology 33:2335–2355.

Dyer, A.D., A.R.H LeBlanc, M.R. Doschak and P.J. Currie. 2021. Taking a crack at the dome: histopathology of a pachycephalosaurid (Dinosauria: Ornithischia) frontoparietal dome. Biosis: Biological Systems 2:248–270.

Evans, D.C., C.M. Brown, M.J. Ryan and K. Tsogtbaatar. 2011. Cranial ornamentation and ontogenetic status of *Homalocephale calathocercos* (Ornithischia: Pachycephalosauria) from the Nemegt Formation, Mongolia. Journal of Vertebrate Paleontology 31:84–92.

Evans, D.C., C.M. Brown, H. You and N.E. Campione. 2021. Description and revised diagnosis of Asia's first recorded pachycephalosaurid, Sinocephale bexelli gen. nov., from the

Upper Cretaceous of Inner Mongolia, China. Canadian Journal of Earth Sciences 58:981–992.

Evans, D.C., S. Hayashi, K. Chiba, M. Watabe, M.J. Ryan, Y.-N Lee, P.J. Currie, K. Tsogtbaatar and R. Barsbold. 2018. Morphology and histology of new cranial specimens of Pachycephalosauridae (Dinosauria: Ornithischia) from the Nemegt Formation, Mongolia. Palaeogeography, Palaeoclimatology, Palaeoecology 494:121–134.

Evans, D.C., R.K. Schott, D.W. Larson, C.M. Brown and M.J. Ryan. 2013. The oldest North American pachycephalosaurid and the hidden diversity of small-bodied ornithischian dinosaurs. Nature Communications 4:1–10.

Gangloff, R.A., A.R. Fiorillo and D.W. Norton. 2005. The first Pachycephalosaurine (Dinosauria) from the paleo-Arctic of Alaska and its paleogeographic implications. Journal of Paleontology 79:997–1001.

Gilmore, C.W. 1924. On *Troodon validus*: an orthopodous dinosaur from the Belly River Cretaceous of Alberta. University of Alberta Department of Geology Bulletin 1:1–43.

Han, F.-L, C.A. Forster, J.M. Clark and X. Xu. 2016. Cranial anatomy of *Yinlong downsi* (Ornithischia: Ceratopsia) from the Upper Jurassic Shishugou Formation of Xingiang, China. Journal of Vertebrate Paleontology. 36:e1029579.

Horner, J.R. and M.B. Goodwin. 2009. Extreme cranial ontogeny in the Upper Cretaceous dinosaur *Pachycephalosaurus*. PLoS ONE 4:e7626.

Jasinski, S.E. and R.M. Sullivan. 2011. Re-evaluation of pachycephalosaurids from the Fruitland-Kirtland transition (Kirtlandian, Late Campanian), San Juan Basin, New

Mexico, with a description of a new species of *Stegoceras* and a reassessment of *Texacephale langstoni*. New Mexico Museum of Natural History and Science Bulletin 53:202–215.

Longrich, N.R., J. Sankey and D. Tanke. 2010. *Texacephale langstoni*, a new genus of pachycephalosaurid (Dinosauria: Ornithischia) from the upper Campanian Aguja Formation, southern Texas, USA. Cretaceous Research 31:274–284.

Maidment, S.C.R. and L.B. Porro. 2010. Homology of the palpebral and origin of supraorbital ossifications in ornithischian dinosaurs. Lethaia 43:95–111.

Maryańska, T. and H. Osmólska. 1974. Pachycephalosauria, a new suborder of ornithischian dinosaurs. Acta Palaeontologica Polonica 30:45–120.

Patterson, C. 1982. Morphological characters and homology. Pp 21–74 in: K.A. Joysey and A.E. Friday (eds). Problems of Phylogenetic Reconstruction, volume 21. London and New York: Academic Press.

Perle, A., T. Maryańska and H. Osmólska. 1982. *Goyocephale lattimorei* gen. et sp. n., a new flat-headed pachycephalosaur (Ornithischia, Dinosauria) from the Upper Cretaceous of Mongolia. Acta Palaeontologica Polonica 27:115–127.

de Pinna M.G.G. 1991. Concepts and tests of homology in the cladistic paradigm. Cladistics 7:367–394.

Schott, R.K. and D.C. Evans. 2012. Squamosal ontogeny and variation in the pachycephalosaurian dinosaur *Stegoceras validum* Lambe, 1902, from the Dinosaur Park Formation, Alberta. Journal of Vertebrate Paleontology 32:903–913.

Schott, R.K. and D.C. Evans. 2017. Cranial variation and systematics of *Foraminacephale brevis* gen. nov. and the diversity of pachycephalosaurid dinosaurs (Ornithischia: Cerapoda) in the Belly River Group of Alberta, Canada. Zoological Journal of the Linnean Society 179:865–906.

Schott, R.K., D.C. Evans, M.B. Goodwin, J.R. Horner, C.M. Brown and N.R. Longrich. 2011. Cranial ontogeny in *Stegoceras validum* (Dinosauria: Pachycephalosauria): A quantitative model of pachycephalosaur dome growth and variation. PLoS ONE 6:e21092.

Schott, R.K., D.C. Evans, T.E. Williamson, T.D. Carr and M.B. Goodwin. 2009. The anatomy and systematics of *Colepiocephale lambei* (Dinosauria: Pachycephalosauridae). Journal of Vertebrate Paleontology 29:771–786.

Sereno, P.C. 2000. The fossil record, systematics and evolution of pachycephalosaurs and ceratopsians from Asia. Pp. 480–516 in: M.J. Benton, M.A. Shiskin. D.M. Unwin and E.N. Kurochkin (eds). The Age of Dinosaurs in Russia and Mongolia. Cambridge: Cambridge University Press.

Simões, T.R., M.W. Caldwell, A. Palci and R.L. Nydam. 2017. Giant taxon-character matrices: quality of character construction remains critical regardless of size. Cladistics 33:198–219.

Sues, H.-D. and P.M. Galton. 1987. Anatomy and classification of the North American Pachycephalosauria (Dinosauria: Ornithischia). Paleontographica Abteilung A 198:1–40.

Sullivan, R.M. 2003. Revision of the dinosaur *Stegoceras* Lambe (Ornithischia, Pachycephalosauridae). Journal of Vertebrate Paleontology 23:181–207.

Sullivan, R.M. 2006. A taxonomic review of the Pachycephalosauridae (Dinosauria: Ornithischia). New Mexico Museum of Natural History and Science Bulletin 35:347–365.

Tsuihiji, T. 2010. Reconstructions of the axial muscle insertions in the occipital region of dinosaurs: Evaluations of past hypotheses on Marginocephalia and Tyrannosauridae using the extant phylogenetic bracket approach. The Anatomical Record 293:1360–1386.

Williamson, T.E. and S.L. Brusatte. 2016. Pachycephalosaurs (Dinosauria: Ornithischia) from the Upper Cretaceous (upper Campanian) of New Mexico: A reassessment of *Stegoceras novomexicanum*. Cretaceous Research 62:29–43.

Williamson, T.E. and T.D. Carr. 2002. A new genus of derived pachycephalosaurian from western North America. Journal of Vertebrate Paleontology 22:779–801.

Woodruff, D.C., M.B. Goodwin, T.R. Lyson and D.C. Evans. 2021. Ontogeny and variation of the pachycephalosaurine dinosaur *Sphaerotholus buchholtzae*, and its systematics within the genus. Zoological Journal of the Linnean Society 193:563–601.